

Structural and Functional Analysis of Intracellular Loop 5 of the NHE1 Isoform of the
Na⁺/H⁺ Exchanger

by

Ka Yee Wong

A thesis submitted in partial fulfillment of the requirements for the degree of

Master of Science

Department of Biochemistry
University of Alberta

© Ka Yee Wong, 2017

Abstract

The mammalian Na⁺/H⁺ exchanger isoform 1 (NHE1) is an integral membrane protein that regulates intracellular pH. It removes a single intracellular proton in exchange for one extracellular sodium ion. It has a large 500 amino acid N-terminal membrane domain that mediates transport and consists of 12 transmembrane segments with several membrane-associated segments including intracellular and extracellular loops. Extracellular regions of this domain are believed to contribute to sodium coordination. Intracellular loops may coordinate protons and modulate the sensitivity to intracellular pH. In this study we characterized the structure and function of intracellular loop 5 (IL5) amino acids Gly431-Lys443. Mutation of eleven residues to alanine caused partial inhibition of transport; notably, mutation of residues R440A and I436A, demonstrated that these residues were critical for NHE1 function. The structure of a peptide of IL5 revealed that it is unstructured in DMSO, however in sodium dodecyl sulfate solution it possessed significant alpha helical character. A significant finding was that Lys438 was in close proximity with Trp434 residue. Overall our results show that IL5 is a critical intracellular loop, with a propensity to form an alpha helix, with many residues being critical for proton transport.

Dedication

To my family: Mom, Dad, Sister, William, and Mr. L

Acknowledgement

First and foremost, my sincere appreciation goes to my supervisor Dr. Larry Fliegel for his guidance and wise suggestions throughout my graduate studies at the University of Alberta. He helped me mature over the course of time with a great deal of patience and tolerance.

Throughout my graduate studies I was granted an opportunity to work with another supervisor, Dr. Ryan T. McKay, an NMR specialist. I would have not been able to make such an accomplishment without his indispensable help with the NMR aspect of my project. I would also like to take the chance to thank my committee members/examiners, Dr. Howard Young, Dr. Brain D. Sykes and Dr. Emmanuelle Cordat for their continuous guidance, constructive feedbacks and criticisms throughout my project.

I must express my particular gratitude to my other mentor, Yong, who shared his vast knowledge on the technical aspect of my project with me. I truly appreciate his wisdom, vigilance and kindness while working under his scrutiny. Also, I would like to thank Xiuju and Deb for being an inspirational role model in the laboratory. My gratitude towards everyone's support is beyond words!

Last but not least, it is my honor to be able to complete my degree at the University of Alberta, a place where I have grown into a reflective and confident individual. Moreover a place where I made many lifelong friendships especially in the Faculty of Medicine. I will never forget this chapter in my life.

Table of Contents

Chapter I:

1. Introduction.....	2
2. Sodium hydrogen exchanger (NHE) family.....	2
2.1. Sodium hydrogen exchanger isoform 1 (NHE1).....	3
2.2. NHE2-10.....	4
2.2.1. NHE2.....	4
2.2.2. NHE3.....	5
2.2.3. NHE4.....	5
2.2.4. NHE5.....	6
2.2.5. NHE6-9.....	6
2.2.6. NHE10.....	7
3. NHE1 topology model.....	7
4. Structure of NHE1.....	13
4.1. Structural analysis of the entire NHE1.....	13
4.2. Selective transmembrane segments of NHE1 determined by NMR spectroscopy.....	14
4.3. Structure analysis of the <i>E. coli</i> sodium proton antiporter by X-ray crystallography	16
4.4. The comparison of EcNhaA and NHE1.....	17
5. How does the Na ⁺ /H ⁺ exchange mechanism work?	18
5.1. NHE1 transport kinetics.....	18
5.2. The exchange mechanism of EcNhaA and NHE1.....	19
5.3. NHE1 regulatory and inhibitory mechanisms.....	20

5.3.1. The N-terminal transmembrane domain of NHE1.....	21
5.3.2. The C-terminal regulatory tail of NHE1.....	21
6. Physiological and pathological roles of NHE1.....	23
7. Functionally critical residues of NHE1.....	25
8. Summary.....	26
9. Thesis objective.....	27

Chapter II: Materials & Methods

1. Materials.....	30
2. Site directed mutagenesis.....	33
3. <i>E. coli</i> transformation.....	34
4. Plasmid isolation.....	34
5. Screening for successful clones by agarose gel electrophoresis.....	35
6. Large scale DNA preparation	36
7. DNA sequencing.....	37
8. Cell culture and stable transfection.....	37
9. Cell culture and transient transfection.....	38
10. Preparation of cell lysates from AP-1 cells.....	39
11. SDS-PAGE and immunoblotting.....	40
12. Na ⁺ /H ⁺ exchange activity.....	43
13. Cell surface expression.....	45
14. Analysis of protein expression levels.....	46
15. Statistics.....	46
16. NMR spectroscopy in deuterated DMSO.....	50

17. NMR spectroscopy in deuterated SDS	50
18. Structure calculations.....	54
Chapter III: Results	
1. Characterization of IL5 mutant proteins.....	59
1.1. Expression levels of IL5 protein mutants of NHE1.....	62
1.2. Surfacing targeting of IL5 mutant proteins of NHE1.....	66
1.3. Activity assay of IL5 mutant protein containing cells.....	71
2. Structural characterization of IL5 protein.....	78
Chapter IV: Discussion	
1. Critical residues of IL5	81
2. Analysis of IL5 structure and function.....	84
Chapter V: Summary.....	88
Chapter VI: Future Directions.....	91
References.....	93

List of Figures:

Chapter I: Introduction

1. Putative topological diagram of NHE1 from Wakabayashi *et al*.....9
2. Putative topological diagram of NHE1 from Landau *et al*.....10

Chapter II: Materials & Methods

3. pYN4⁺ plasmid template.....32
4. Sample of activity trace of Na⁺/H⁺ exchanger assay.....42
5. 1D Spectra of IL5 in 440mM of SDS (A) NOESY (B) TOCSY.....48
6. Ramachandran plot for IL5 protein.....53

Chapter III: Results and Discussion

7. A topological model of the IL5 of the transmembrane domain of the NHE1 isoform of the Na⁺/H⁺ exchanger.....56
8. Alignment of amino acid sequence of IL5 and surrounding region of various NHE1 proteins.....58
9. NHE1 protein expression of AP-1 cells stably transfected (A) and transiently transfected (B) with wild type or mutant NHE1.....60
10. NHE1 protein surface localization of AP-1 cells stably transfected (A) and transiently transfected (B) with wild type or mutant NHE1.....64
11. Rate of pH_i recovery from and acute acid load by AP-1 cells stably transfected (A) and transiently transfected (B) with wild type or mutant NHE1.....68
12. Temperature titration of 2.8 mM of DMSO.....73
13. Temperature titration of 440 mM of SDS.....74
14. IL5 in different orientations showing hydrophobicity.....75

15. Electrostatic potential maps of IL5 peptide.	76
16. Structural characteristics of IL5.....	77

Chapter IV: Discussion

17. 1D Spectra of IL5 in ~2.8 mM of DMSO (A) and 440mM of SDS (B) solution.	83
---	----

List of Tables:

Chapter II: Materials & Methods

1. Oligonucleotide primers for site-directed mutagenesis.....31
2. CYANA 2.1 statistics for IL5 peptide structural calculations.52

Abbreviations

12CA5	Anti-HA antibody
Alpha-MEM	Modified eagle's medium, alpha modification
Amp	Ampicillin
AP-1	Chinese hamster ovary cell line deficient in plasma membrane Na ⁺ /H ⁺ exchanger
ATP	Adenosine 5'-triphosphate
BCECF	2'.7'-bis(carboxyethyl-5 (and 6)-carboxy) fluorescein
BCECF-AM	2'.7'-bis(carboxyethyl-5 (and 6)-carboxy) fluorescein acetoxymethyl ester
BGS	Bovine growth serum
bp	Base pair
BSA	Bovin serum albumin
CAII	Carbonic anhydrase II
CaM	Calmodulin
CCL39	Chinese hamster lung fibroblast
cDNA	Complementary DNA
CH ₃ COOH	Acetic acid
CHO	Chinese hamster ovary cells
CHP1	Calcineurin homologous protein 1
CHP3	Tescalcin

C-terminal	Carboxy terminal
CYANA	Combined assignment and dynamics algorithm for NMR applications
DAG	Diacylglycerol
DIDS	diisothiocyanostilbene-2,2'-disulfonic acid
DMSO	Deuterated dimethylsulfoxide
DNA	Deoxyribonucleic acid
DPC	Dodecylphosphocholine
ECL	Enhanced chemiluminescence
EcNhaA	<i>E. coli</i> Na ⁺ /N ⁺ antiporter
<i>E. coli</i>	Escherichia coli
EDTA	Ethylenediaminetetraacetic acid
EGF	Epidermal growth factor
EIPA	5-(N-ethyl-N-isopropyl) amiloride
EL	Extracellular loop
ERM	Ezrin, radixin, and moesin
G418	Geneticin
GAM	Goat anti-mouse
HA	Hemagglutinin
HEPES	N-2-hydroxyethylpiperazine-N'2-ethanesulfonic acid
HOE642	Cariporide
HOE694	3-methylsulfonyl-4-

	piperidinobenzoyl guanidine
IL	Intracellular loop
IP	Immunoprecipitation
IP3	inositol 1,4,5-triphosphate
KDa	Kilodalton
LB	Lysogeny broth
LF2000	Lipofectamine™ 2000 reagent
MEM	Minimum essential medium
MMP	Metalloproteases
Nha	Sodium/proton antiporter
NHE	Sodium/proton exchanger
NHE1	Sodium /proton exchanger isoform 1
NMR	Nuclear magnetic resonance
NRVM	Neonatal rat ventricular myocytes
N-terminal	Amino terminal
PBS	Phosphate buffered saline
PCR	Polymerase chain reaction
pHi	Intracellular pH
PIP ₂	Phosphatidylinositol 4, 5-bisphosphate
SDS	Deuterated sodium dodecyl sulfate
SDS-PAGE	Sodium dodecyl sulfate polyacrylamide gel

	electrophoresis
S.E.	Standard error
TBS	Tris-buffered saline
TE Buffer	Tris and EDTA buffer
TROSY	Transverse relaxation optimized spectroscopy
TM	Transmembrane
WT	Wild type

Chapter I Introduction

1. Introduction

The mammalian Na^+/H^+ exchanger type I isoform (NHE1) is ubiquitously expressed as a plasma membrane protein and catalyzes the removal of a single intracellular proton in exchange for a single extracellular sodium ion (1). NHE1 is a transport protein and its purpose is to regulate pH, volume and cation gradients in cells (2). The maintenance of intracellular pH (pH_i) is critical for cellular functions. Failure to regulate pH_i may alter the expression of normal and pathological genes that result in disease (2,3). Together, the regulation of pH_i , volume and cation gradient in cells contributes to optimal cell growth and cell viability. Plasma membrane proteins are important and worthwhile to study because they make up 20-30% of the genome of the organism and are critical to cell growth and function (4). Here we focus on resolving part of NHE1 protein structure and examining which residues are critical. This information may ultimately assist in drug development and therapeutics (5).

2. Sodium hydrogen exchanger (NHE) family

There are many different types of Na^+/H^+ exchangers (NHE) that exist in different isoforms in all living things (6). All NHEs serve a similar purpose, that is to catalyze the transmembrane (TM) exchange of Na^+ for H^+ . In eukaryotes, NHEs play a greater role in regulation of intracellular pH while in prokaryotes they are more involved in exporting Na^+ for salt tolerance. There are three cation/proton antiporter families, CPA1 (fungi, plants, and mammals), CPA2 (*E. coli* NhaA, yeast sod2, human Nha1 and Nha2) (6,7) and a Na^+ transporting carboxylic acid

decarboxylase family (mammalian sperm-specific NHEs) (6). In my thesis, I focus on mammalian NHE1. There are nine well known mammalian sodium proton exchanger isoforms. Although a tenth isoform has been discovered, more studies are needed to confirm its function (8,9). Each isoform is believed to have the same membrane topology (an N-terminal 12 TM segments and a C-terminal regulatory tail) however they differ in tissue, cellular location and regulation (10).

2.1. Sodium hydrogen exchanger isoform 1 (NHE1)

Murer *et al.* were the first group to discover mammalian NHE protein in rat intestinal and renal microvilli (11). After the initial findings, Pouyssegur *et al.* explored the first known isoform of the mammalian NHE protein and postulated a Na^+/H^+ exchange mechanism. NHE1 was found to be an important pH_i regulator, and four main properties of NHE1 were found. 1. The transport of NHE1 protein was dependent on Na^+ or Li^+ . 2. Amiloride and its analogues could inhibit NHE1 protein. 3. Growth factors can activate NHE1 protein. 4. The proton gradient serves as a driving force (12). The amino acid sequence of NHE1 was first predicted based on the cDNA sequence by Sardet *et al.* in 1989. To gain a greater understanding of how the NHE1 protein regulates pH, Sardet *et al.* cloned and expressed the mammalian NHE1 protein and investigated its function, kinetics, regulation, expression, structure and localization (13). The putative structure of NHE1 was also hypothesized. They predicted a N-terminal TM domain of 500 residues that is responsible for cation translocation ($1\text{Na}^+:1\text{H}^+$) and pH sensing. The other end of NHE1 protein was a C-terminal regulatory domain with 315 residues in the

cytoplasm that regulates NHE1 activity. Na^+/K^+ ATPase was suggested to provide the energy for transport by making the sodium electrochemical gradient (14). In total, the NHE1 protein is made up of 815 amino acids (2). The NHE1 protein is ubiquitous and it resides in the plasma membrane and basolateral membrane of polar cells (1,2). NHE1's role depends on the location of tissue. For example, NHE1 in the myocardium it is involved in diseases such as hypertension, cardiac hypertrophy, myocardial ischemia and reperfusion injury (15). It is also a trigger for metastasis in breast cancer (16). In clinical studies it has been shown that the absence of NHE1 in mice can lead to ataxia, seizure and growth retardation (17).

2.2. NHE2-10

2.2.1. NHE2

As mentioned above, there are other isoforms of sodium proton exchangers and each isoform resides in different locations and has different functions. By screening libraries of different species using mammalian NHE1 cDNA probes (9), other isoforms were identified and it was found that NHE1-NHE8 were highly homologous (18). NHE2 is predominantly found on the apical membrane of epithelial cells in colon, kidney, skeletal cells and to a lower level in testis, ovary and small intestine (19,20). NHE2 was found to have an amino acid sequence that was 42% identical to NHE1 (21). NHE2 regulates steady-state pH_i and cell volume in rat cortical collecting duct cell line. Its activity is more responsive to intracellular acidosis (22). Similar to NHE1, NHE2 cation translocation activity is inhibited by amiloride and 5'-amino alkyl substituted derivatives (19,20). In mice, NHE2 does

not play a role in acid secretion on the gastric epithelium of parietal cells; however, NHE2 is essential for development and viability (23). In the absence of NHE2, gastric parietal cells showed a net decrease in acid secretion compared to the wild type (23).

2.2.2. NHE3

NHE3 was found to have an amino acid sequence that was 39% identical to NHE1 (23). NHE3 is predominantly found on the apical membrane of epithelial cells in colon, small intestine and kidney (24,25). Its role in intestine and colon is to reabsorb Na^+ and water into epithelial cells (26). In the kidney, it is also important in reabsorbing Na^+ and NaHCO_3 where NHE3 couples with the Cl^- /base, formate or oxalate exchangers (27). The proton gradient that is created by NHE3 generates a proton motive force for other transporters (28,29). When NHE3 is absent in mice, they experience diarrhoea, a decrease in blood pressure and an acidic plasma pH (23). Unlike NHE2, NHE3 is unresponsive to inhibitors such as amiloride and its derivative (30,31). NHE3 is predominantly found in kidney and the intestine.

2.2.3. NHE4

NHE4 was shown to have an amino acid sequence was 42% identical to NHE1 (32). NHE4 is predominantly found in the basolateral membrane of gastrointestinal tract cells and is present in a minor amount in the kidney, brain, skeletal muscle, heart, uterus and liver (33-35). NHE4 is a unique isoform of NHE as NHE4 is resistant to amiloride and ethylisopropylamiloride inhibition. It was

reported that (DIDS) has the ability to activate NHE4 that is stably transfected in fibroblasts (36,37). This is surprising since DIDS is an inhibitor of anion exchangers (38). Mice with deleted NHE4 experienced reductions in acid secretion, loss of parietal and mature chief cells, and showed elevated amounts of undifferentiated, necrotic and apoptotic cells (39). Therefore, NHE4 is necessary for normal gastric secretion, cell growth, and development in mice (39).

2.2.4. NHE5

NHE5 was found to have an amino acid sequence that was 39% and 53% identical to NHE1 and NHE3, respectively (32). NHE5 is predominantly found in the plasma membrane and recycling endosomes of brain cells (40,41). Secretory carrier membrane proteins bind to the N- and C-terminal of NHE5 directly (41). Similar to NHE3, NHE5 is unresponsive to inhibitors such as amiloride compounds and its derivative (31,42). In clinical studies, NHE5 is involved in end-stage renal disease and Familial Paroxysmal Kinesigenic Dyskinesia (43,44).

2.2.5. NHE6-9

NHE6 and NHE9 are exclusively found in the membranes of intracellular vesicles such as early and late endosomes respectively (34,45), and also highly expressed in brain specifically hippocampus and cortex (46). NHE7 and NHE8 are found in the membranes of mitochondria such as trans-golgi network and mid-golgi network respectively (45). The absence of NHE6 can lead to a neurological disease called Angelman syndrome (47). NHE6-9 is associated to neurological conditions

such as autism, attention deficit hyperactivity disorder, intellectual disability and epilepsy (46). The function for NHE6-9 is to maintain an optimal pH in intracellular (45) and to regulate cation (Na^+ , K^+) in organelle systems (golgi bodies and endosomes) (46). The absence of NHE6 and NHE9 cause hyperacidification of endosomal lumen (46).

2.2.6. NHE10

NHE10 is a unique isoform, in terms of function and location. Although it has a very similar predicted topology to NHE1, the sequence identity of NHE10 to the other NHE isoforms is very low (approximately 12 – 14%) (8). NHE10 is found in osteoclasts and does not function to regulate pH_i (8). Similar to isoforms NHE6 to NHE9, there are many studies yet needing to be done.

3. NHE1 topology model

Earlier studies of Sardet *et al.* used hydropathy analysis and predicted the membrane domain consisted of 500 residues with ten TM segments (48,49). They found that the residue Asn75 acts as a N-linked glycosylation site (50). Also, the C-terminal tail was predicted to be in the intracellular compartment and was thought to be important for phosphorylation regulation (51,52). Another group, Orłowski *et al.* supported the findings by Sardet *et al.* that NHE1 had ten TM segments by analysis of sequence alignment of NHE1-4 from rat (53). However, the predicted model of Orłowski *et al.* slightly differed from Sardet *et al.*'s model where they disagreed with the assignment of the first two TM segments.

The summary of the early predictions for the mammalian NHE1 protein was that it consists of a N-terminal domain of ten TM segments that are connected by a series of intracellular loops (IL) and extracellular loops (EL). The TM segments were thought to be responsible for cation translocation. Two potential glycosylation sites were suggested and a long hydrophilic C-terminal cytosolic tail of 315 amino acids has binding sites for lipid, proteins and sites of phosphorylation by kinases (48). In total, the NHE1 protein has 815 amino acids with an apparent molecular weight of 110 kDa in the mature glycosylated protein (48,54).

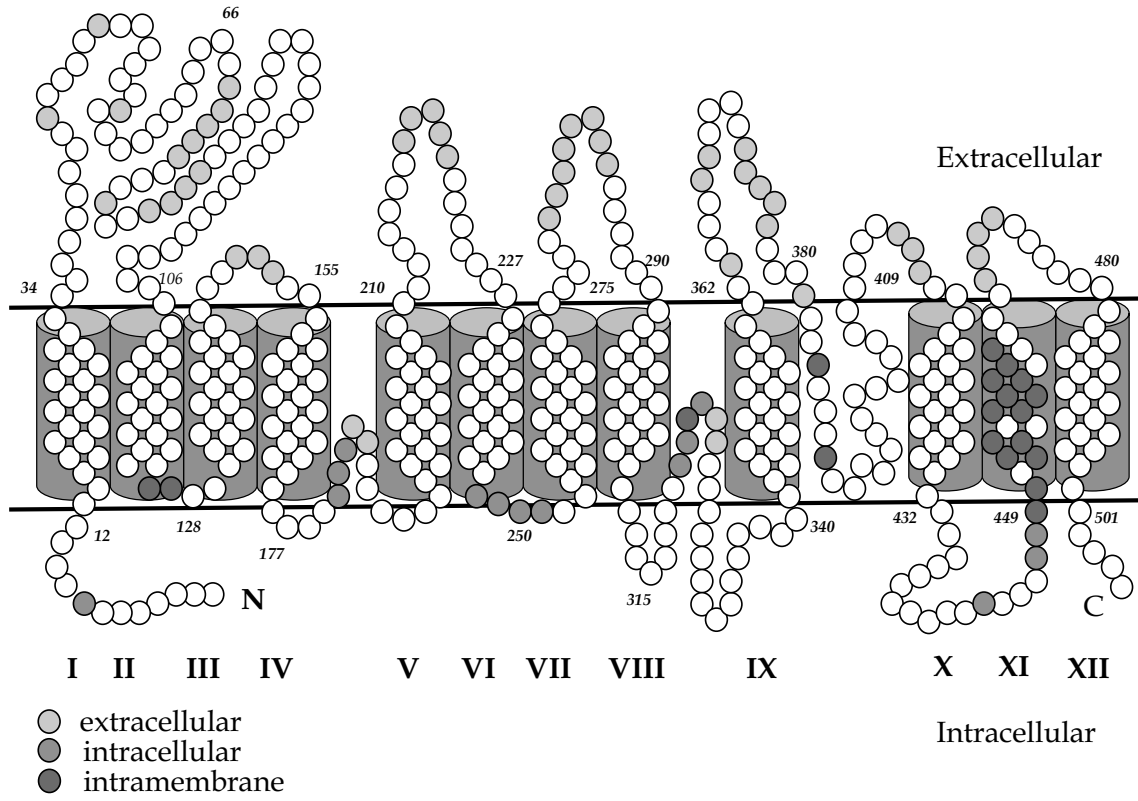
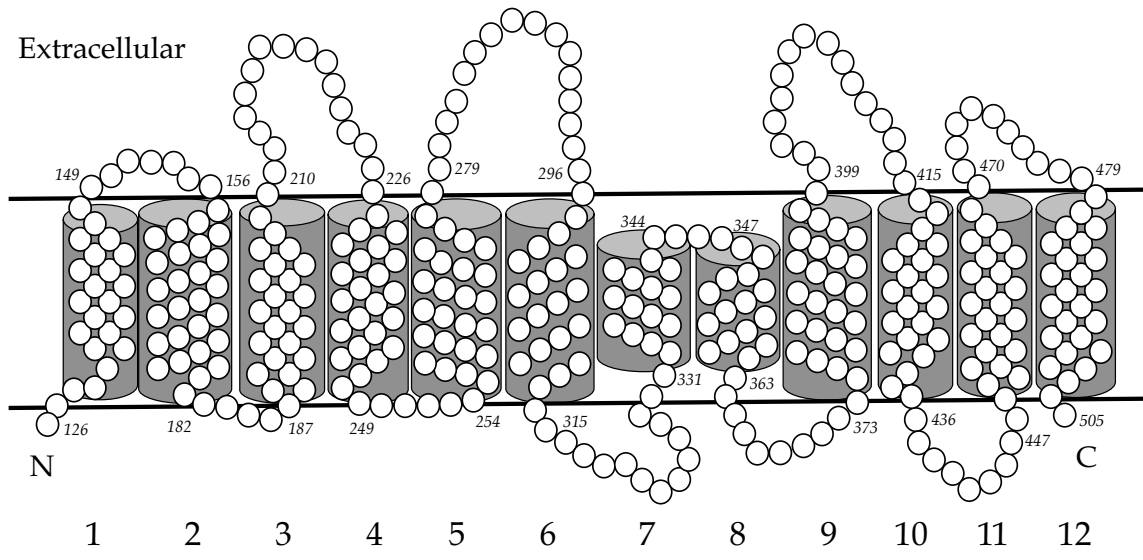


Figure 1. Putative topological diagram of NHE1 from Wakabayashi *et al.*

adapted from (55)



Intracellular

Figure 2. Putative topological diagram of NHE1 from Landau *et al.* adapted from (56)

In 2000 Wakabayashi *et al.* (57) proposed a more detailed topology (see Figure 1) and another newer model was proposed seven years later by Landau *et al.* (56,58) (see Figure 2). Wakabayashi *et al.* deduced the topology of NHE1 by substituted cysteine accessibility analysis (57). Briefly, residues on the EL and IL were mutated to cysteine. They examined the accessibility of the cysteines to the sulfhydryl reactive reagents to determine the orientation and configuration of NHE1 TM segments. When cysteine residues were labeled with biotin-maleimide, those were designated as being in the extracellular compartment. In contrast, intracellular cysteine residues were not labeled with both biotin-maleimide applied externally to the cells. Aside from the determination of ELs and ILs, Wakabayashi *et al.*'s NHE1 topology model proposed 12 TM segments (average of 21 – 22 residues per segment), which differed from the predicted structure of ten TM segments described earlier. Wakabayashi *et al.* identified both the N- and C- terminal ends as intracellular. In addition, three re-entrant loops were proposed between TMIV and TMV (intracellular side), TMVIII and TMIX (intracellular side), and TMIX and TMX (extracellular side) and they may play a role in ion transport.

Landau *et al.* had a different approach, which came after the publication of *E. coli* Na⁺/H⁺ antiporter (EcNhaA) crystal structure (56,58). Landau *et al.* constructed a 3D-model of NHE1 using sequence alignment and the EcNhaA crystal structure as templates. It was found that the sequence identity of NHE1 and EcNhaA was only approximately 10% (56). The predicted structure of NHE1 was suggested by evolutionary conservation analysis (56). The new topology model was very similar to the previous Wakabayashi's model where it consisted of 12 TM segments with a

large C-terminal tail starting at the 506th residue (56,58). Four important differences from Wakabayashi's model were observed. Landau's model did not have any re-entrant loops (intracellular loops that dipped into the membrane bilayer) and TMI commences at a different location. For Wakabayashi's model, TMI started at His13 whereas for Landau's model TMI started at Val129. Also Landau *et al.* suggested that the first two TM segments did not contribute to cation exchange activity because they were poorly conserved (54). In the new model, TMVII and TMVIII were only 14 residues long and that is shorter than the average length of TM segments of 21-22 residues (50,59). Furthermore, the new model suggested that the two intracellular loops in the region of residues 176-189 and 320-330, contained amino acids that reside in the membrane as loops. In contrary to the first model, the region of residues 176-189 and 320-330 are intracellular loops in the cytoplasm (60). In addition to these differences, Landau *et al.* suggested that signal peptides were present in the first two TM segments of NHE1. Topology studies on NHE1, NHE3 and NHE6 showed that in the first hydrophobic segments there was a signal peptide (61,62). Furthermore, with the program SignalP tools, NHE2, NHE4 and NHE5 were predicted to contain signal peptides. Also Landau *et al.* proposed that the region of residues 315-411 forms a three TM segments (56) which is in contrary to Wakabayashi's model.

Recently in 2015, Liu *et al.* found that the region of residues 1-127 forms two TM segments and are not cleaved as a signal peptide. In addition, the region of residues 315-411 were found to form a TM segment by cysteine scanning

accessibility (63). This finding agrees completely with the first model by Wakabayashi *et al.* and strongly disagrees with Landau's initial proposal.

4. Structure of NHE1

It is important to understand the structure of a membrane protein because it is closely related to the molecular mechanism of transport. In 1975, the structure of bacteriorhodopsin, a membrane protein, was first investigated by low-resolution electron spectroscopy (64). A decade later, the photosynthetic reaction center structure was revealed by a high-resolution X-ray spectroscopy (65). Due to the extensive study of membrane proteins, it is now known that membrane proteins typically follow the “positive inside rule”, that is that positively charged residues reside in the intracellular loops (66). Moreover, an “aromatic belt” is observed, where a greater portion of aromatic residues reside on the membrane solvent interface (67). Another important property of membrane proteins is their structural features that are important for protein function such as proline-induced kinks, re-entrant loops and discontinuous helices (68,69).

Until now, the high-resolution crystal structure of NHE1 has not been available but to gain a better understanding of the secondary and tertiary structure of NHE1, many different biochemical and spectroscopic techniques such as NMR spectroscopy, electron microscopy and circular dichroism spectroscopy are currently reported (53,70,71).

4.1. Structural analysis of entire NHE1

The entire NHE1, consisting of 815 amino acids, was overexpressed and purified from *Saccharomyces cerevisiae* and examined under an electron microscope at a resolution of 22 Å (70). NHE1 was shown to be a homodimer (of two compact higher density regions of two NHE1 monomers) in proteoliposomes with a dimension of 100 Å x 100 Å x 90 Å (70). This was confirmed by size-exclusion chromatography, with NHE1 showing a molecular weight of NHE1 ~220 kDa as a dimer (70). Stable dimers at 220 kDa and monomers at 110 kDa of NHE1 have also appeared on the SDS-PAGE (72-74). Two intrinsic cysteines Cys561 and Cys794 on the cytoplasmic regulatory tail contribute to dimer formation (74). This structural analysis revealed that the cytoplasmic domain contributes to intermolecular contact and stabilization. Furthermore, by circular dichroism spectroscopy, the overall framework for the secondary structure of NHE1 was found to be 41% alpha helical, 23% beta sheet, and 36% random coil (70).

4.2. Selective transmembrane segments of NHE1 determined by NMR spectroscopy

Although X-ray crystallography is a very useful method for the structural determination of NHE1, NMR spectroscopy is an alternative approach which does not need crystal formation and is non-invasive. Another useful advantage of NMR spectroscopy is that a dynamic structure is allowed, whereas X-ray crystallography provides a snap-shot static image. Additionally, the very nature of membrane proteins makes it difficult to form crystals for crystallographic analysis. However, a weakness for NMR is the size limitation. A typical NMR instrument has a size

limitation of ~20 kDa proteins (75) and a highly purified protein is usually required. Although, currently ~50 kDa proteins can be resolved by a TROSY (transverse relaxation optimized spectroscopy), however this is still a protein size limitation (76). The entire NHE1 is nearly impossible to be solved by standard liquid NMR due to the complexity of assignments, size of protein, and basic physical limits of NMR.

In previous studies, NMR spectroscopy was used to determine the structures of the following TM segments (TMIV, TMVII, TMIX, and TMXI of NHE1) (57,71,77-79) and the TM segments structure was determined in various solvent systems. The solvent system CD₃OH: CDCl₃: H₂O was used for TMIV produced in *E. coli*. By NMR spectroscopy, it was found that the region of residues 159-163 and 165-169 forms a coil and extended segment respectively. The residues in the region 174-175 and 169-176 form a beta-turn and a short alpha-helical region respectively (80). Residues in the region (251-273) of TMVII were made synthetically and analyzed by NMR in dodecylphosphocholine (DPC) micelles (79). It was found that TMVII is primarily alpha helical with extended N- and C-terminal regions. A region in TMVII (Gly261 and Glu262) is not alpha helical which is predictable because it is known that glycine residues are TM segments helix breakers (81). Similar to TMVII, TMIX (339-363) was also synthetically made and analyzed in DPC micelles. It was observed that TMIX possesses a L-shaped conformation. The N- and C-terminal helix regions at residues 340-344 and 353-359 respectively were connected by a large kink at Ser351 that bent the TMIX to approximately a 90° angle (82). Similar to TMVII and TMIX, TMXI (449-470) was synthetically made and analyzed in DPC micelles. It appeared that the N- and C-terminal residue regions (447-454) and

(460-471) respectively were helical and TMXI is also a discontinuous segment. With similar reasoning, the separation was due to two glycine residues (78).

4.3. Structure analysis of the *E. coli* sodium proton antiporter by X-ray crystallography

The crystal structure of the *E. coli* Na⁺/H⁺ antiporter (EcNhaA) was first solved at a resolution of 3.45 Å by X-ray crystallography (58). By sequence alignment, EcNhaA and NHE1 are only 10% identical (6). The stoichiometry of EcNhaA Na⁺/H⁺ is 1Na⁺:2H⁺ (electrogenic) which differs from NHE1 with 1Na⁺:1H⁺ electroneutral exchange. The direction of cation movement is also opposite of one another. In addition, EcNhaA is activated by an alkaline pH whereas NHE1 is activated by an acidic pH (58,83). Despite those differences, both NHE1 and EcNhaA belong to the same cation/proton antiporter superfamily and the two cations that are involved in translocation are Na⁺ and H⁺ for both transporters (6). EcNhaA allows survival in sodium containing external environments (84,85). Even though the crystal structure of EcNhaA showed 12 TM segments, there are only 388 residues and an absence of a C-terminal regulatory domain. EcNhaA has less amino acids than NHE1's 815 amino acids, and it consists of two three-TM segments bundles, namely, TM3-TM5 and TM10-TM12. EcNhaA also has two discontinuous TM segments, TM4 and TM11 with wide openings facing the intracellular and extracellular compartment (58). TM4/M11 cross over each other at their extended regions in an anti-parallel orientation. Important features of EcNhaA are the Asp133 (negatively charged residue) lying in between the positive helix dipoles and

the Lys300 (positively charged residue) lying in between the negative helix dipoles. Both residues Asp133 and Lys300 compensate for Coulomb repulsion (the repulsive force between two positive and two negative charges) by the breaks in TM4/TM11 (58). It is interesting that the residues (Asp163 and Asp164 on TM5) that coordinate the translocation of cations in EcNhaA, are in close proximity to the TM4/TM11 assembly (58). As mentioned above, the disadvantage of X-ray crystallography is that protein must be crystallized and this requires it to be in an inactive state which occurs at pH 4. Perhaps due to this, it was seen that the center pore of EcNhaA was narrow and a continuous pore was not visible (58).

4.4. The comparison of EcNhaA and NHE1

The Landau *et al.* homology model was comparable to EcNhaA, especially, the core of NHE1 which is more conserved (56). The most conserved TM segments, when comparing NHE1 and EcNhaA are, TMII (2), TMIV (4), TMV (5), TMVIII (8), and TMXI (11). The TM segments of TMIV (4) and TMXI (11) assembly underlay the core of an alternating-access mechanism.

There are two components to the alternating-access mechanism, the unwinding of TM segments and the cation translocation. In EcNhaA, an assembly of the TM4 and TM11 both unwind to form extended peptides overlapping one another in the center of the TM segment. Two titratable residues located on residue Asp133 of TM4 and residue Lys300 of TM 10, stabilize these two irregular TM segments. Asp133 and Lys300 in EcNhaA are conserved to Asp238 and Arg425 in NHE1. Two glycine residues were found in TMXI of NHE1 and were predicted to facilitate the

unwinding of TMXI. The ion transport path is responsible for the cation translocation that is formed by two funnels in EcNhaA. One funnel that is made up of TM2, TM4, TM5 and TM9 opens to the cytoplasmic part. The other funnel that is made up of TM2, TM8 and TM11 opens to the periplasm. Both funnels do not form a continuous pore because of the restriction in the middle of the plasma membrane near the TM4/TM11 assembly (56). However, this conformation responds to pH activation and allows the translocation of cations (58). Since the TM4/TM11 assembly and the critical residues in EcNhaA involved are highly conserved to NHE1, the TMIV/TMXI assembly and alternating access mechanism of NHE1 is believed to behave in a similar manner (56).

5. How does the Na⁺/H⁺ exchange mechanism work?

The secondary active transporter, NHE1 is an electroneutral transporter where a Na⁺ exchanges for a H⁺. The movement of a Na⁺ down its electrochemical gradient provides the energy for H⁺ extrusion (86). The Na⁺ gradient plays a role in determining the direction of cation exchange (87). The activity of NHE1 is induced by acidic pH_i and at pH 6.5, NHE1 activity is at its maximum (88). Interestingly, NHE1 also has the ability to translocate a Li⁺ for an intracellular H⁺ (34,60,88)

5.1. NHE1 transport kinetics

NHE1 becomes active at an acidic pH_i and is at maximum, or near maximum activity at a pH of 6.5 NHE1. Meanwhile at a physiological pH_i of ~7.2, NHE1 remains dormant. The kinetics of NHE1 follows the Monod-Wyman-Changeux

model that explains that the molecular transitions in NHE1 are induced by the presence of H^+ and intracellular activating signals (3,89,90). NHE1, as a homodimeric membrane protein, has transport affinities that are dependent on the intracellular H^+ (89,90). There are two states, the higher and the lower affinity states. The lower affinity state is inactive and is favored by equilibrium during physiological pH ~ 7.2 . In contrast, the higher affinity state (an active) state is favored by an equilibrium during an acidic pH ~ 6.5 (91). It was proposed that there are two protonation sites and a cooperative regulation of a dimeric NHE1 protein (89). It is known that with the absence of the C-terminal region of NHE1, dimerization ceased and the rate of cation transport decreased by approximately 10-fold (74).

5.2. The exchange mechanism of EcNhaA and NHE1

The cation exchange mechanism was analyzed from the crystal structure of EcNhaA antiporter (92) and by computational simulation (93,94). The three components of EcNhaA that are responsible for cation exchange are TM4 and TM11, Asp163-Asp164 on TM5 that bind to cations and TM9 that plays a role in pH_i sensing (58). TM9 acts as a pH sensor and reacts to a high pH_i with a conformational shift. This induces the opening of an intracellular facing funnel formed by TM4 and TM11 (58). At this configuration, the Na^+ binding site of Asp163-Asp164 on TM5 is exposed. The binding of Na^+ to the binding site causes an imbalance of charges and initiates a movement in the flexible loops of the TM4/11 assembly (58). The translocation of Na^+ is aided by a series of conformational changes in the TM

segments where Asp163-Asp164 expels a Na⁺ to the periplasm. Immediately, two H⁺'s bind to Asp163-Asp164 from the periplasm and are delivered to the cytoplasm with the aid of TM4/11 assembly (58). The antiporter quickly reverts back to its resting state and a Na⁺ binds again and the translocation repeats (58).

The cation translocation mechanism proposed by Landau *et al.* (based on the homology model structure of NHE1), is very similar to the cation translocation mechanism analyzed in the EcNhaA antiporter (56). Similarly, TMIV/TMXI are thought to be responsible for the opening and closing of funnels. However, instead of Asp163-Asp164, it is Asp267 that is responsible for the binding of H⁺ and Na⁺. Upon intracellular acidosis, NHE1 experiences a conformational change. Where TMIV/TMXI opens up the cytoplasmic funnel and exposes Asp267 for protonation (56). Once the H⁺ binds to Asp267, a series of conformational changes eventually forms an extracellular funnel. Ultimately, the H⁺ gets off loaded from Asp267 and Asp267 and they pick up a Na⁺ simultaneously. Again, a conformational change results in bringing the Na⁺ to the intracellular compartment. The antiporter reverts back to its resting state and the transport of H⁺ and Na⁺ repeats (56).

5.3. NHE1 regulatory and inhibitory mechanisms

It is necessary to understand the NHE1 regulatory mechanism in order to develop drugs for the therapeutics for cancer and cardiac disease. The exploration of inhibitory mechanisms is necessary to gain a better understanding of how to make new improved inhibitors of the protein.

5.3.1. The N-terminal TM domain of NHE1

The N-terminal TM domain contains the binding regions for inhibitors such as amiloride and cariporide. Moreover, in TM segments, TMIV and TMIX contain inhibitor binding sites (95). Specifically, mutation of Phe165 and Leu167 of TMIV and Glu350 and Gly356 of TMIX alters inhibitor sensitivity suggesting they are part of, or near, the inhibitor binding site (96,97). Amiloride is not a very effective inhibitor but a derivative of it, EIPA is greatly increased in potency and specificity. The benzoylguanidines inhibitors, cariporide (HOE642 and HOE694) are more effective inhibitors than amiloride (95). An attempt was made in earlier clinical trials to use cariporide to treat cardiac ischemia and reperfusion injury. However, the outcome was not significant partially because of a lack of specificity and partially due to the method of administration of the compound. Hence, further work on drug development is needed (98,99). Aside from inhibitors, there are stimulators of NHE1 such as epidermal growth factor, thrombin, serum, insulin, and lysophosphatidic acid and angiotensin-II (34,52,87,100,101).

5.3.2. The C-terminal regulatory tail of NHE1

The C-terminal tail of NHE1 is responsible for regulation. Signaling molecules, hormones, secondary messengers, kinases, lipids and adaptor proteins tightly regulate NHE1 activity (15). There are six key players that are involved with the regulation of NHE1 at the C-terminal. Phosphatidylinositol 4,5-bisphosphate (PIP₂) is a signaling lipid in the plasma membrane that affects NHE1 function. The activity of kinases and phosphatases affect the PIP₂ concentration, which is directly

affected by ATP concentrations (102). It is known that NHE1 does not consume ATP, however NHE1 is reduced by ATP depletion (103). Experimental evidence that supports the link between NHE1 and PIP₂ is the mutation of the two PIP₂ binding sites at residues 513-520 and 556-564 of NHE1. This reduces Na⁺/H⁺ exchange activity (104). Another experiment showed that decreasing intracellular ATP and decreasing PIP₂ binding both lowered the cation exchange activity and ion transport rate (105). In summary, NHE1 and PIP₂ work closely together and affect the cation exchange activity and ion transport (105).

Calcinuerin B homologous protein 1 (CHP1) binds to NHE1 in a Ca²⁺ - dependent manner. CHP1 stimulates NHE1 activity (106-108). Calmodulin (CaM) is another protein that binds in a Ca²⁺ -dependent manner, and it is capable of binding to two sites: a high affinity site at residues (636-656) and a low affinity site at residues (657-700) (109). CaM binding removes the effects of an auto-inhibitory by binding to the high affinity CaM site (109).

Tescalcin (CHP3) also belongs to the CHP family. The relationship of CHP3 with WT NHE1 protein and mutant NHE1 protein were examined. The outcome was that although the NHE1 mutant proteins were targeted to cell surface, the activity was remarkably reduced. Surprisingly, the expression of CHP3 in the WT mutant protein up-regulated cell surface activity. It is now known that CHP3 promotes the biosynthetic maturation and half-life at the cell surface and hence contributes to a functional NHE1 protein at the cell surface (110).

The enzyme carbonic anhydrase II (CAII) is a catalyst that aids the formation of H⁺ and HCO₃⁻ from the reactant CO₂. CAII directly interacts with the NHE1 C-

terminal tail at amino acids 790-802 (104,111). Since CAII is a catalyst, it helps to increase the rate of formation of H⁺'s, which are a substrate of NHE1 (112). ERM (Ezrin/Radixin/Moesin) proteins serve as a linker that connects the actin filaments close to the plasma membrane. Together actin filaments and ERM proteins assist NHE1 in modulating cell migration and maintain the cell structure (113,114).

6. Physiological and pathological roles of NHE1

Beyond the regulation of pH_i, NHE1 is indirectly involved in many physiological and pathological roles. Physiologically, it facilitates inward sodium flux in response to osmotic shrinkage, also the promotion of differentiation and cell growth (115), and enhances cell motility (116). A hypertonic environment induces osmotic shrinkage and NHE1 is activated (117). The activity of NHE1 generates an intracellular sodium ion gradient that is coupled to the osmotic movement of water into the cell (118,119). During cell differentiation and development, the expression level of NHE1 varies (120-123). In mouse studies, NHE1 activity is compulsory for the development of stem cells and differentiation of cardiomyocytes.

The relationship between NHE1 and cell growth was first investigated by Pouyssegur *et al.* (124). They used the NHE deficient Chinese hamster lung fibroblast cell line (CCL39). Their observations showed that at a pH_i less than 7.2, the growth of NHE deficient CCL39 cells is greatly hindered. In contrast, normal cells were able to grow at a pH range of 6.6 to 8.2. Therefore, it is known that NHE is involved in the regulation of pH_i for optimal cell growth and

differentiation (124). The activity of NHE1 also contributes to cell motility. Migration of cells depends on cytoskeletal protein actin filaments where an alkaline pH_i can lead to actin polymerization (125). The C-terminal regulatory tail NHE1 contains a binding site for ERM proteins (Ezrin/Radixin/Moesin), which is responsible for aiding in cell migration (114,126,127).

In pathology, NHE1 is important in breast cancer cell invasiveness. NHE1 activity enhances invasion by breast cancer cells by raising pH_i and acidifying extracellular microenvironment of tumour cells (128-131). An experiment showed that in mice, the WT CCL39 cell line (NHE1 containing) was more prone to carcinogenic invasion than the NHE deficient CCL39 cells (132). This may be because extracellular acidification facilitates protease activation such as for matrix metalloproteases (MMPs). Also intracellular alkalinisation caused by NHE1 can elevate the expression of MMPs and vascular endothelial growth factor (133,134). They facilitate the digestion and remodelling of the extracellular matrix that is critical in metastasis (135,136).

NHE1 is also involved in the myocardium in another pathological role. It promotes heart hypertrophy and amplifies the damage that occurs during myocardial ischemia and reperfusion. During cardiac ischemia-reperfusion, insufficient oxygen supply to cells induces anaerobic respiration and this produces lactic acid and protons. Ultimately, the intracellular acidification activates NHE1 (137,138). When NHE1 is active, it exchanges a Na^+ for every H^+ getting expelled and this accumulates Na^+ in the intracellular compartment. This will eventually generate a sodium gradient that provides a driving force

for reverse mode of the $\text{Na}^+/\text{Ca}^{2+}$ exchanger. The influx of Ca^{2+} eventually reaches the threshold to initiate a cascade of cellular events that ultimately lead to cell injury, apoptosis and necrosis (48,137,139,140).

In preclinical trials, it has been proven that inhibition of NHE1 protects the myocardium from ischemia-reperfusion damage (141-144). However, clinical trials did not show the same result, possibly due to a lack of specificity of the inhibitors (145). A deeper understanding of the structure and the function of NHE1 can facilitate the development of more specific inhibitors for clinical use.

7. Functionally critical residues of NHE1

The characterization of NHE1 is important in order to gain a better understanding of how NHE1 functions. This is accomplished by mutation and truncation analysis. The type of mutational analysis used includes cysteine scanning mutagenesis, alanine scanning mutagenesis and charge reversal mutagenesis. Ultimately, we seek a better understanding of how cations are being translocated by the TM segments, how NHE1 responds at different pH_i 's and how dimerization and surface targeting of NHE1 protein to the membrane are regulated. Previously in Wakabayashi's topology model, Phe161 (TMIV), Leu255 and Leu258 (TMVII), Glu346 and Ser351 (TMIX), and Leu457, Ile461 and Leu465 in (TMXI) are pore lining residues, they were found by cysteine scanning mutagenesis and sulfhydryl reactive compounds (79,82,124).

Mutation of some residues such as Phe161-Leu163, Ile169, Ile170 and Gly174, has the capability of affecting the efficacy of the inhibitors amiloride and cariporide (96,97,146,147). By cysteine and alanine scanning mutagenesis, it was found that the residue, Asp267 is a putative protonation site in the cation translocation pore of NHE1. Asp267 also was important for cation transport activity (79,148). NHE1 lost its function in pH sensing in the absence of ATP when residues 516-590 were deleted (149). Therefore, the residues in the region 516-590 of the C-terminal tail were important in this regard. Individual residues such as Arg440 in intracellular loop 5 (IL5), Gly455 and Gly456 in TMXI were putative pH sensing amino acids. An acidic shift resulted when Arg440 was mutated to R440C, R440H, R440D, R440L, R440E. An alkaline shift resulted when Gly455 was mutated to bulky amino acids (150).

There were residues that, when mutated, caused NHE1 to fail in targeting to the plasma membrane. NHE1 residues, Leu156, Asp159, Pro156, Pro168, Asp172, Gly309, Ile451, Tyr454, Gly455, Gly456, Arg458 and Gly459 were individually mutated to cysteine. These mutant proteins failed to mature and to target to the plasma membrane surface, and these mutant proteins were pH unresponsive (73,78,151). This was further confirmed by immunofluorescence microscopy because, both T454C and R458C were retained in the endoplasmic reticulum (152). Remember that NHE1 loses its pH regulatory ability when it fails to target to the plasma membrane.

8. Summary

The mammalian NHE1 protein consists of 12 TM segments, a N-terminal and a long regulatory cytosolic tail. These TM segments are connected by a series of IL and EL and the loops are significant because their presence can influence the arrangement and packing of TM segments (153). In addition, they can modulate protein function (154). EL of NhaA contains critical residues for pH induced activation (155) and dimerization (156). Murtazina *et al.* found that in the EL re-entrant loop between TM IX and TMX contained a critically important residue, E391, that was important for activity (157). EL2 contains residues critical for inhibitor binding (158). Wang *et al.* found a critical residue, C477, in EL6 that is functionally important in NHE1 (159).

9. Thesis objective

Previous studies in the Fliegel lab have mostly examined EL's such as EL5. Mutations in EL5 resulted in changes in drug sensitivity and cation binding (160,161). EL2 links TM segments I and II and mutations of residues of EL2 have been shown to affect both the drug sensitivity and the activity of NHE1 (162,163). There were two models of NHE1 structure. One based on cysteine accessibility studies by Wakabayashi *et al.* (55) and a second based on computational comparison with the deduced structure of the *E. coli* Na⁺/H⁺ exchanger NhaA by Landau *et al.* suggested (56). However, recently we demonstrated that the model based on cysteine accessibility is correct with

regard to C-terminal part of the membrane domain (63). Both models place amino acids of IL5 in an intracellular location.

Recently a study (164) has demonstrated that some individual changes to charged amino acids in IL, can affect NHE1 function. It is also known that mutation to these charged residues can shift the pH_i dependence of the exchanger (150,165,166). With the knowledge that these regions are important in NHE1 function, we used a combination of two approaches to study the region, IL5. NMR was used to characterize the structural properties of a synthetic peptide of IL5, and site specific mutagenesis was used to characterize the functional role of amino acid residues of IL5 (amino acids 431-443). We present here the first results of the complete analysis of IL5 and confirm that a number of the residues of this region are important in NHE1 function.

Chapter II Materials and Methods

1. Materials

The IL5 sequence (acetyl⁴³¹GLTWFINKFRIVK⁴⁴³-amine) used in this study was commercially obtained from Biomatik. NMR tubes were obtained from Norell Inc. (Norell 502). PWO DNA polymerase was from Roche Molecular Biochemicals, Mannheim, Germany. SulfoNHS-SS-biotin was from Pierce, Rockford, IL, USA. LIPOFECTAMINE™ 2000 Reagent was from Invitrogen Life Technologies, Carlsbad, CA, USA. Anti-HA-antibody was from Santa Cruz Biotechnology (Santa Cruz, CA). BCECF-AM was from Molecular Probes, Inc. (Eugene, OR). Restriction enzymes were purchased from New England Biolabs (Ontario, Canada) and Invitrogen. All other chemicals were of analytical grade and were purchased from Fisher Scientific (Ottawa, ON), Sigma or BDH (Toronto, ON).

Mutation	Sequence	Restriction Site
G431A	5' CGCGTGCTGGGGGT GCTaGc CCCTGACCTGGTTCATCAAC3'	<i>NheI</i>
L432A	5' CTGGGGGTGCTGGG Cgcc ACCTGGTTCATCAAC3'	<i>NarI</i>
T433A	GCTGGGGGTGCTGGG gCTag CCTGGTTCATCAACAAG3'	<i>NheI</i>
W434A	5' CGTGCTGGGGGTGCT aGGCCT GACCgcGTTTCATCAACAAGTCC3'	<i>StuI</i>
F435A	5' GTGCTGGGCCTGACCTGGgc CATtAA tAAGTTCGGTATCGTGAAGCTG3'	<i>AseI</i>
I436A	5' GGCCTGACCTGGT TCgcg AACAAGTTCGGTATC3'	<i>NruI</i>
N437A	5' CTGACCTGGTTCAT TCgcg AAGTTCGGTATCGTG3'	<i>NruI</i>
K438A	5' GACCTGGTTCATCA ACgc GTTCGGTATCGTGAAGC3'	<i>MruI</i>
F439A	5' GGTTCATCAACAAGgcCCGTATCGT GAAGCTt ACCCCAAGGACCAG3'	<i>HindIII</i>
R440A	5' GTTCATCAACAAGTTCgc ATCGT GAAAGCTGACC3'	<i>PvuI</i>
I441A	5' CTGGCCTGACCTGGTTC ATtAA tAAGTTCGGTgcCGTGAAGCTGACCCCAAG3'	<i>AseI</i>
V442A	5' CAACAAGTTCGGTATCgc GAAGCTt ACCCCAAGGACCAG3'	<i>HindIII</i>
K443A	5' CAAGTTCGGTATCGT agcGCT GACCCCAAGGACCAG3'	<i>AfeI</i>
K438D	5' GTGCTGGGCCTGACCTGGTTC ATtAA tgacTTCGGTATCGTGAAGCTGAC3'	<i>AseI</i>
R440D	5' GGTTCATCAACAAGTTC gaTATCGT GAAAGCTGACCCCAAG3'	<i>EcoRV</i>

Table 1. Oligonucleotide primers for site-directed mutagenesis.

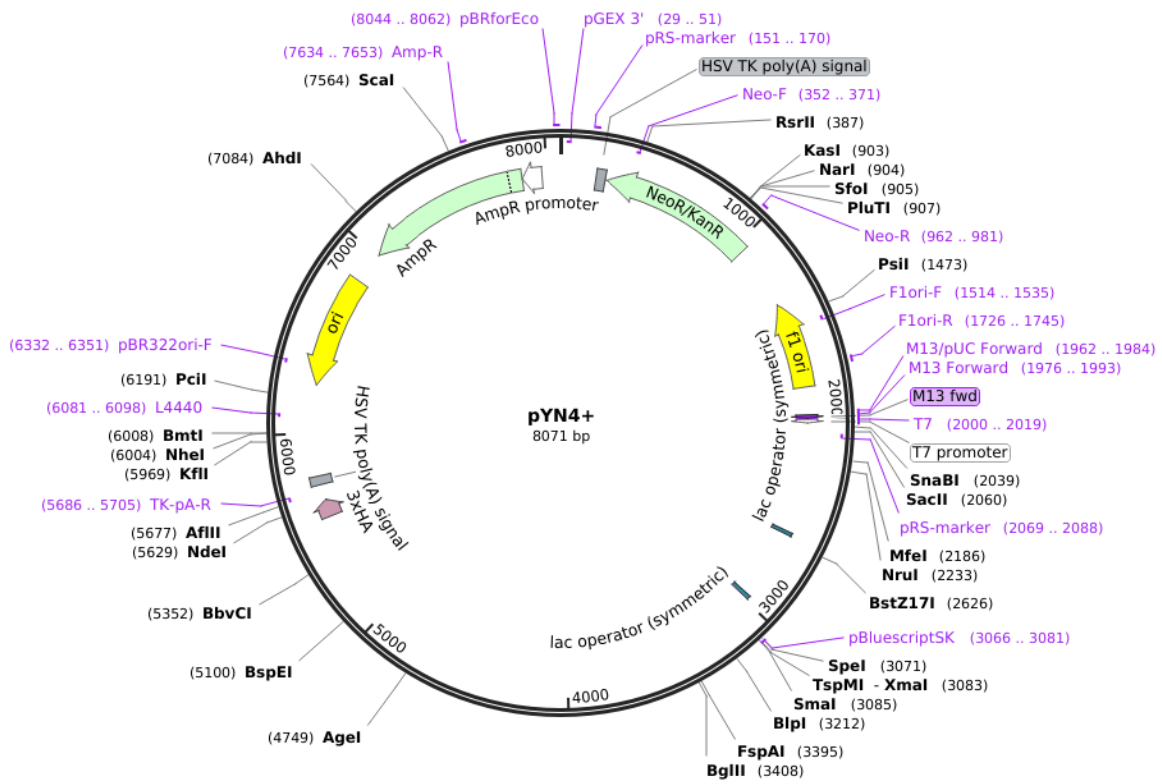


Figure 3. pYN4+ plasmid template (167).

2. Site directed mutagenesis

Alanine scanning mutagenesis was used for each residue of IL5 from Gly431 to Lys443. Lys438 and Arg440 were mutated to aspartate acid. All mutations were designed to create or remove a new restriction enzyme site for use in screening transformants (see Table 1). Mutations were made to an expression plasmid (pYN4⁺) containing a tagged, human NHE1 isoform of the Na⁺/H⁺ exchanger. Figure 3 shows the plasmid pYN4⁺ contains the cDNA of the entire coding region of human NHE1. It has a C-terminal hemagglutinin (HA) tag that we have previously shown does not affect activity (167).

Polymerase chain reaction (PCR) was used for site directed mutagenesis of NHE1 IL5. The plasmid pYN4⁺ containing cNHE1 was denatured at 60° for 15 minutes prior to addition of PCR reaction solutions. The subsequent experiments were performed on ice. Two sample mixtures, A and B, were prepared in microfuge tubes. Tube A consisted of: 5 µL of 2.5 nM dNTP mix (dATP, dTTP, dCTP, dGTP), 9 µL of ddH₂O, 1 µL of plasmid template at 0.75 µg/µL, 5 µL of 10 µM forward primer and 5 µL of 10 µM reverse primers. Tube B has the following contents: 19.5 µL ddH₂O, 5 µL PWO buffer and MgSO₄ and 0.5 µL PWO polymerase. Prior to incubation in the Techne Thermal Cycler TC-312, tube A and tube B were combined together. The PCR consisted of 18 cycles. Each cycle has the following steps: a denaturing step at 95° for 30 seconds, an annealing step at 55° for one minute and an elongation step at 68° for 20 minutes. PWO DNA polymerase (Roche Molecular Biochemicals, Mannheim, Germany) was used for amplification and site-directed

mutagenesis was performed using Stratagene (La Jolla, CA, USA) QuikChange™ site directed mutagenesis kit as recommended by the manufacturer.

3. *E. coli* transformation

Once the PCR products were obtained, they were digested with the enzyme *DpnI* for 4-5 hours at 37°. *DpnI* was purchased from Invitrogen, Carlsbad, Ca, USA. The digested product (about one to three µL) was transformed via electroporation into electrocompetent *E. Coli* DH5α™ competent cells. Cells were left to recover in 500 µL lysogeny broth (LB) medium 37° for an hour. Finally, the transformed cells were placed on LB agar plates (15 g of bacto agar in 1.0 L LB medium and 50 µg/mL ampicillin) 0.15 µg/L and the plates were incubated overnight at 37°.

4. Plasmid isolation

E. coli colonies appeared on the LB ampicillin plates after 14-16 hours of incubation at 37°. Single *E. coli* colonies were selected and cultured overnight in 1.5 mL LB at 37° with agitation. Plasmids were isolated by following DNA extraction protocols (Invitrogen Life Technologies, Carlsbad, CA, USA). Cells were collected by centrifugation at 10 000 rpm for three minutes. Cell pellets were re-suspended in 150 µL P1 buffer (50 mM Tris pH 8.0, 10 mM EDTA, 100 µg/mL RNase) and incubated at room temperature for ten minutes. 150 µL of P2 lysis buffer (200 nM NaOH, 1% SDS) was added to the mixture and thoroughly mixed until the lysate turned viscous. 150 µL of P3 neutralization buffer (3 M CH₃COO 1.5% glacial acetic acid) at 4° was added, briefly mixed and placed on ice for ten minutes. To remove

the white fluffy precipitates that contained genomic DNA, proteins and cell debris were centrifuged at 14 000 rpm for five minutes. The pellet was discarded and the supernatant was transferred to a new microfuge tube. 150 μ L of phenol-chloroform (25 phenol:24 chloroform:1 isoamyl alcohol) was added to extract plasmid DNA. The mixture was vortexed and centrifuged at 14 000 rpm for five minutes. Heterogeneous fractions resulted and only the top aqueous layer was transferred into a new microfuge tube. The plasmid DNA was then precipitated in 1 mL cold 100% EtOH at -20° for at least 20 minutes and centrifugation at 14 000 rpm for five minutes. The DNA pellet was rinsed with 70% EtOH and dissolved in 50 μ L of ddH₂O.

5. Screening for successful clones by agarose gel electrophoresis

Not all isolated plasmids contained the desired mutation. It was necessary to screen for the introduced mutations by restriction enzyme digestions using the appropriate added or deleted sites. The putative mutant plasmids (5 μ L) were added into a reaction mixture containing the following: 1 μ L of restriction enzyme, 0.5 μ L of 1 mg/mL RNase, 0.2 μ L BSA, 2 μ L of 10X reaction buffer and ddH₂O was added to a total of 20 μ L. This reaction mixture was incubated at 37° for two hours. To separate the DNA fragments, a 1% agarose gel containing 0.5 mg/mL ethidium bromide was used. To estimate the size of the DNA, a 1kb DNA ladder (Invitrogen Life Technologies, Carlsbad, CA, USA) was loaded into a separate lane of the gel. After electrophoresis, the agarose gel was viewed under UV light with a UV-transilluminator and pictures were taken with a regular digital camera.

6. Large scale DNA preparation

Upon isolation of mutant containing DNA, a large-scale preparation of DNA was made. This purification from *E. coli* was carried out by using QIAGEN plasmid maxi kit and followed the manufacturer's protocol. Positive mutants were cultured overnight in 150 mL LB containing 286 μ M of ampicillin. The cells were harvested by centrifugation at 6000 g for 15 minutes at 4°. Pellets were re-suspended in 10 mL of cold P1 buffer (50 mM Tris/Cl pH 8.0, 10 mM EDTA, 100 μ g/mL RNase A, 1 μ L Lyseblue/ P1 mL). 10 mL P2 (200 mM NaOH, 1% SDS (w/v)) was added immediately and mixed gently until the lysates turned blue. The mixture was allowed to sit for no more than five minutes at room temperature. 10 mL of P3 (3 M CH₃COOK pH 5.0) at 4° was added and the mixture was incubated on ice for 20 minutes. To remove most of the precipitates (containing genome DNA, proteins and cell debris) that formed in the mixture, the sample was centrifuged was at 20 000 g for 30 minutes at 4°. A second centrifugation followed at 20 000 g for 15 minutes at 4° to remove remaining precipitates. The supernatant was loaded in a QIAGEN-tip 500 equilibrated in the same buffer. This allowed binding of plasmid DNA to the column. The column was washed twice with 30 mL QC buffer (1.0 NaCl, 50 mM MOPS pH 7.0, 15% isopropanol (v/v)) and eluted with 15 mL QF buffer (1.25 NaCl, 50 mM TrisCl pH 8.5, 15% isopropanol (v/v)). Plasmid DNA was precipitated with 10.5 mL isopropanol and centrifuged at 15 000 g for 30 minutes at 4°. DNA pellets were rinsed with 70% EtOH and allowed to air dry. 400 μ L of TE buffer (10 mM Tris, 1 mM EDTA) was added to re-dissolved plasmid.

7. DNA sequencing

Plasmids acquired from QIAGEN Maxi-kit were sequenced to confirm mutation sites. A sample of 260 nM concentration of plasmid DNA and a 2 pmol/ μ L of primer, approximately 100 base pair upstream of mutation site, were used for sequencing. All DNA sequencing was performed at the University of Alberta, Department of Biochemistry, DNA Core Services Laboratory.

8. Cell culture and stable transfection

Stable cell lines of WT and all mutants plasmids (except W434A) were made by transfecting WT and mutant plasmids into AP-1 cells via transfection with LIPOFECTAMINE™ 2000 Reagent (LF2000) (Invitrogen Life Technologies, Carlsbad, CA, USA). LF2000 is typically used for protein expression with high transfection efficiencies. AP-1 Cells are a Chinese hamster ovary (CHO) cell line that lacks an endogenous Na⁺/H⁺ exchanger (168). Prior to transfection, AP-1 cells were cultured in 60 mm dishes with a α -MEM medium (Hyclone, Logan, UT, USA) containing 10% BGS, and 25 mM HEPES without any antibiotics. When AP-1 cells achieved 90% confluence, 4 μ g of wild type or mutant plasmids were used for transfection. The 20 μ L of LF2000 was diluted in 500 μ L of Opti-MEM medium and incubated for five minutes at room temperature. Then 4 μ g of plasmids were combined with the LF2000 and Opti-MEM mixture for 20 minutes to allow the formation of DNA-LF2000 complexes. During this time, AP-1 cells were washed with phosphate buffered saline (PBS) (contains KH₂PO₄, NaCl, and Na₂HPO₄·7H₂O) changed to α -MEM medium that contained neither antibiotics nor bovine growth serum. PBS is a

balanced salt solution used for washing cells. Afterward the DNA-LF2000 complex solution was added to AP-1 cells. This transfection took place in an atmosphere of 5% CO₂ and 95% air. After 4-6 hours, 10% BGS was added and cells were incubated in 5% CO₂ and 95% air at 37° until the next day.

AP-1 cells were split into 3 plates at three different dilutions of 1:10, 1:50, and 1:100 in a α -MEM supplemented with 10% (v/v) bovine growth serum, 25 mM HEPES, penicillin (100 U/mL) and streptomycin (100 μ g/mL). Initially, 800 μ g/mL of geneticin (G418) was added to the cultures to select for positively transfected cells for three consecutive days. Fresh α -MEM medium was changed each day until the third day, α -MEM medium was changed every other day until colonies began to form and G418 was decreased to 600 μ g/mL. When the appearance of colonies was prominent, G418 was further decreased to 400 μ g/mL up until 2 to 3 days before isolation of single colonies. Cell colonies were isolated with a sterile pipette and transferred to a 12-well plate with 1.5 mL α -MEM containing 5% BGS with 400 μ g/mL G418. The medium was changed the next day to α -MEM containing 400 μ g/mL G418 and fresh medium was replaced every 2 to 3 days. When the post transfected cells became confluent, they were trypsinized and transferred into a 35 mm dishes and a 6-well plate. Cells in 35 mm dishes were used to check for NHE1 expression and cells in 6-well plates were used as stable cell lines and stored in liquid nitrogen tank in CryoTube™ vials (NUNC™, Denmark) for future use.

9. Cell culture and transient transfection

WT and mutant plasmid, W434A were made by transfecting WT and mutant plasmids into AP-1 cells via transfection with LIPOFECTAMINE™ 2000 Reagent (LF2000) (Invitrogen Life Technologies, Carlsbad, CA, USA). LF2000 is typically used for protein expression with high transfection efficiencies. AP-1 Cells are a Chinese hamster ovary (CHO) cell line that lack an endogenous Na⁺/H⁺ exchanger (168). Prior to transfection, AP-1 cells were cultured in 60 mm dishes with a α -MEM medium (Hyclone, Logan, UT, USA) containing 10% BGS, and 25 mM HEPES without any antibiotics. When AP-1 cells achieved 90% confluence, 4 μ g of wild type or mutant plasmids were used for transfection. The 20 μ L of LF2000 were diluted in 500 μ L of Opti-MEM medium and incubated for five minutes at room temperature. Then 4 μ g of plasmids were combined with the LF2000 and Opti-MEM mixture for 20 minutes to allow the formation of DNA-LF2000 complexes. During this time, AP-1 cells were washed with phosphate buffered saline (PBS) (contains KH₂PO₄, NaCl, and Na₂HPO₄·7H₂O) changed to α -MEM medium that contained neither antibiotics nor bovine growth serum. PBS is a balanced salt solution used for washing cells. Afterward the DNA-LF2000 complex solution was added to AP-1 cells. This transfection took place in an atmosphere of 5% CO₂ and 95% air. After 4-6 hours, 10% BGS was added and cells were incubated in 5% CO₂ and 95% air at 37° until the next day.

10. Preparation of cell lysates from AP-1 cells

Cell lysates were harvested from 35 mm dishes when confluence reached 80-90%. Plates were placed on ice to reduce protein degradation. Growth medium was

removed by aspiration and cells on the plate were washed with 4° PBS, RIPA lysis buffer (1% NP-40, 0.25% sodium deoxycholate, 0.1% Triton X-100, 5 mM EDTA, 0.1 mM PMSF, 0.1 mM benzamidine, lab-made protease inhibitor cocktail) was added to the plates for three minutes. A sterile disposable cell scraper was used to scrap off the cells and the lysates were transferred into microfuge tubes. To remove cell debris, samples were centrifuged at 14 000 rpm for five minutes at 4°. Supernatants were kept in microfuge tubes for later analysis by SDS-PAGE.

11. SDS-PAGE and immunoblotting

Western blot analysis was used to confirm NHE1 expression (169) and SDS-PAGE 10% acrylamide gels were used. A single lane was reserved for protein standards. Each sample contained 100 µg of cell lysate and 4X SDS-loading buffer (30% glycerol, 3% 2-mercaptoethanol, 6% SDS, 0.13 M Tris pH 6.8, 0.133 g/mL bromophenol blue). Each loaded sample was incubated at 37° for ten minutes and the maximum loading volume was 60 µL. Samples ran for 40 minutes at 70 V in the stacking gel and one hour at 120 V in the separating gel layer.

Upon completion of SDS-PAGE, the separating gel containing the resolved NHE1 and other proteins were transferred onto a nitrocellulose membrane (Bio-Rad Laboratories, Ontario, Canada) for 2 hours at 450 mA. The stacking gel was discarded. After transfer of proteins onto the nitrocellulose membrane, the membrane was blocked with a 10% milk solution: 1 g/10 mL, Tris- buffered solution, *i.e* TBS, 50 mM Tris and 150 mM NaCl, with agitation for 1-2 hours at room temperature. Primary antibody, 12CA5 (1:2000 dilution monoclonal mouse anti-HA

antibody) was added overnight at 4° with agitation in TBS in the presence of 1% milk. After primary incubation, the nitrocellulose membrane was washed with TBS 4 times, 15 minutes each time. For secondary antibody incubation, GAM (1:10 000 dilution, Goat-Anti-Mouse) was added and incubated for 1-2 hours at room temperature in TBS and the presence of 1% milk. The Amersham enhanced chemiluminescence western blotting and detection system was used to detect immunoreactive proteins. After the secondary incubation, the nitrocellulose membrane was washed 4 times with TBS for 15 minutes each time. Afterwards the nitrocellulose membrane was immersed in 10 mL of ECL reagent (Tris-HCl pH 8, 22.5 mM luminol, 6 mM commaric acid and 0.04% hydrogen peroxide) for one minute. Development of X-ray films (Fuji medical X-ray film) was carried out using a Kodak X-OMAT 2000 M35 processor. ImageJ 1.35 software (National Institutes of Health, Bethesda, MD, USA) was used to quantify band intensities.

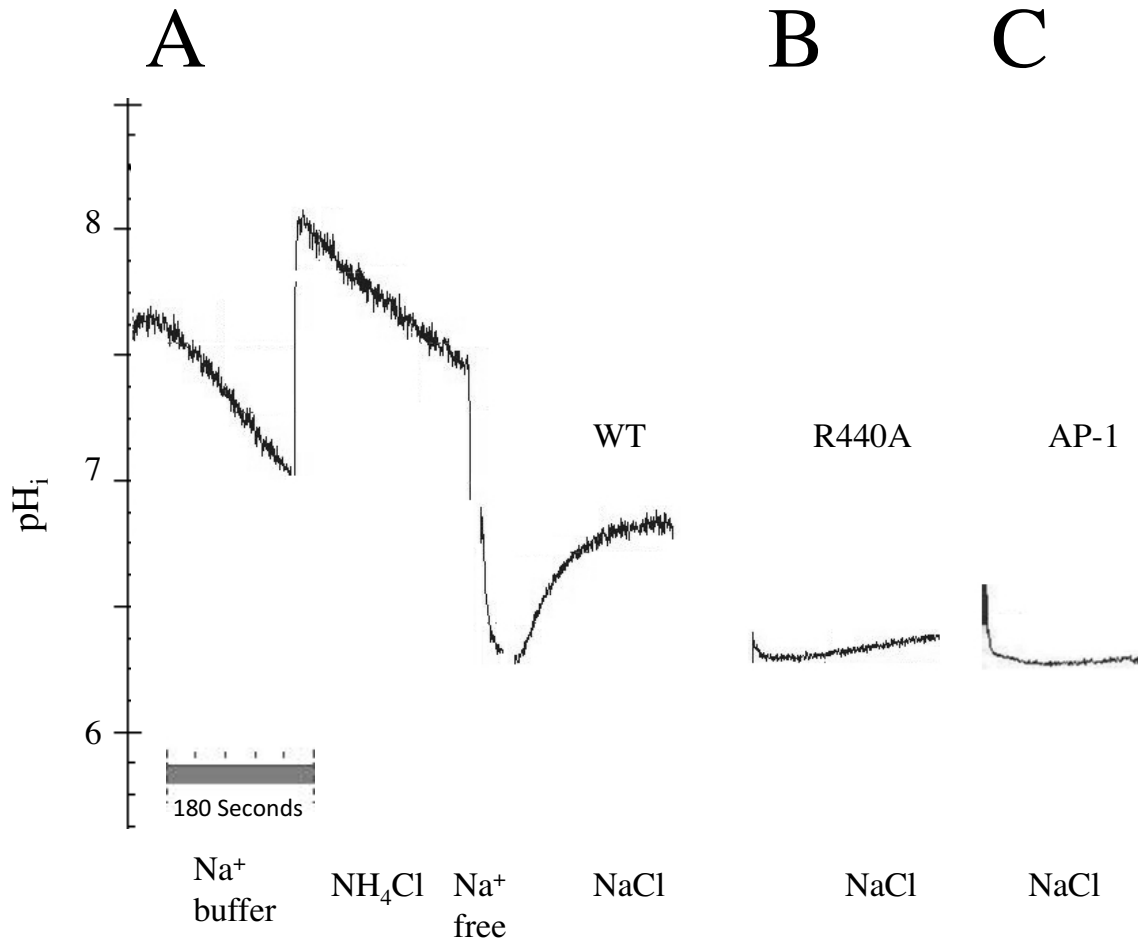


Figure 4. NHE1 protein activity was assayed in stably transfected AP-1 cells. Cells were in Na^+ buffer for three minutes. Then were treated with NH_4Cl for three minutes, after the NH_4Cl treatment, there was a brief Na^+ containing free treatment to induce acidosis. This was followed by a treatment in Na^+ containing buffer to induce NHE1 activity. A three-point pH calibration at pH 8, 7, and 6 was performed after every assay. **A.** WT NHE1 (positive control). **B.** R440A mutant protein **C.** AP-1 cell (negative control).

12. Na⁺/H⁺ exchange activity

NHE1 activity was measured using a PTI Deltascan spectrofluorometer. Stably transfected cells were placed on glass coverslips (2×10^5 cells per coverslip, Thomas Red label micro cover glasses) and grown until they reached 80-90% confluence. At least two independently made clones of each IL5 mutant stable cell line were made. Experiments were performed at 37°. Prior to the activity assay, WT and mutants grown on coverslips were incubated at 37° in α -MEM medium overnight. On the day of the activity assay, the coverslips were incubated in 400 μ L serum free α -MEM medium containing 1.875 μ g/mL of 2',7-bis (2-carboxyethyl)-5-caboxyfluorescein-AM (BCECF-AM); Molecular Probes Inc., Eugene, OR, USA) for 20 minutes to allow BCECF-AM to permeate through the cell membrane. The fluorescence of BCECF varies with pH. BCECF-AM is non-fluorescent and permeable to the cell membrane. However, once inside a cell, de-esterification occurs by intracellular esterases and BCECF-AM becomes BCECF which is impermeable and trapped inside the cell. A dual excitation single emission ratiometric method of BCECF was used to allow for the correction of the absolute level of fluorescence, which varies with the amount of BCECF absorbed. Therefore, BCECF treated cells were excited at both 425 nm and 503 nm and the ration of emission was measured at 524 nm.

To measure the activity of NHE1, cells were transiently acidified using 50 mM ammonium chloride (NH₄Cl). Ammonium chloride is added to the solution containing the coverslips. Ammonium (NH₄⁺) enters the cell and dissociates into ammonia (NH₃⁺) and proton (H⁺). After equilibrium is established, external

ammonium chloride is removed by changing solutions. Since ammonia is small and uncharged, it can readily diffuse out of the cell more rapidly than ammonium. By Le Chatelier's principle, this changes the equilibrium to the product side and more H^+ is produced, therefore inducing intracellular acidosis.

After the incubation with BCECF-AM the coverslip was transferred to a cuvette holder with constant stirring at 37° . It was incubated in 2.5 mL "Normal buffer" containing 135 mM NaCl, 5 mM KCl, 1 mM $MgCl_2$, 1.8 mM $CaCl_2$, 5.5 mM glucose, and 10 mM Hepes, pH 7.4 at 37° for three minutes. Normal buffer is nominally bicarbonate free. Intracellular acidosis was induced by adding 50 μ L of 2.5 M ammonium chloride to the normal buffer in the cuvette and cells were incubated for another three minutes. Followed by withdrawal for 30 seconds in "Na⁺ free buffer": (135 mM *N*-methyl-*D*-glucamine, 5 mM KCl, 1 mM $MgCl_2$, 1.8 mM $CaCl_2$, 5.5 mM glucose, and 10 mM Hepes, pH 7.4). The removal of the external ammonium chloride in sodium free buffer induced transient intracellular acidification because without Na⁺, NHE1 was unable to recover the pH_i of cells. Finally, intracellular pH (pH_i) recovery was in "Normal buffer" for at least three minutes. NHE1 protein activity was determined using the slope of the first 20 seconds of the recovery period.

Following pH_i recovery for every experiment, a three-point pH calibration curve was made using the K^+ /nigericin method with Na⁺ free calibration buffers (135 mM *N*-methyl-*D*-glucamine, 5 mM KCl, 1 mM $MgCl_2$, 1.8 mM $CaCl_2$, 5.5 mM glucose, and 10 mM Hepes, pH 6, 7, 8) and 10 μ M nigericin. Nigericin is an ionophore that equilibrates K^+ and H^+ across the cell membrane. Because we earlier found that

growth conditions affect the absolute level of NHE1 activity, experiments comparing the activities of wild type and NHE1 mutants were done in pairs grown to the same degree of confluence and with the same media. Figure 4 shows the sample of activity trace of Na⁺/H⁺ exchange assay with intracellular acidosis treatment procedure.

13. Cell surface expression

Cell surface expression was measured to determine the degree to which all mutant proteins were targeted to the cell surface. Cells were grown to 50-70% confluence in 35 mm dishes. Growth medium was removed by aspiration and cells were washed with 4° phosphate buffer saline (PBS). This was followed by a second wash with 4° with borate buffer pH 9.0 (154 mM NaCl, 7.2 mM KCl, 1.8 mM CaCl₂, and 10 mM boric acid). Cells were labeled with 3 mL Sulpho-NHS-SS-Biotin (Pierce Chemical Company, Rockford, IL, USA) at a concentration of 0.5 mg/mL in borate buffer and cells were incubated for 30 minutes at 4°. Afterward, cells were washed three times with quenching buffer pH 8.3 (192 mM glycine and 25 mM Tris) at 4°. Solubilization of cells was achieved by addition of 500 µL immunoprecipitation lysis buffer pH 7.5 (1% (w/v) deoxycholic acid, 1% (w/v) Triton X-100, 0.1 (w/v) SDS, 150 mM NaCl, 1 mM EDTA, 10 mM Tris/Cl, 0.1 mM PMSF, 0.1 mM Benzamidine, and a protease inhibitor cocktail). To remove cell debris, the sample was centrifuged at 16 000 g at 4° for 20 minutes. The pellet was discarded and supernatants were obtained and transferred into two equal 200 µL fractions in microfuge tubes. One of the tubes was labeled as “Total” fraction and the other tube was labeled was

“Unbound” fraction. In the unbound fraction, 50 μ L of immobilized streptavidin resin was used to remove surface labeled protein. Unbound fractions were then incubated at 4° overnight with gentle rocking. The total fraction was stored in -20° freezer. The following day, the tube that contained the unbound fraction was centrifuged at 16 000 g for two minutes. The pellet was discarded and supernatants, consisted of unbounded proteins were used for SDS PAGE. Equal amounts of the total and unbound proteins were analyzed by 10 % SDS-PAGE followed by western blotting against the HA tag and quantification using Image J software. Relative amounts of NHE1 on the cell surface were calculated by comparing both the 110 kDa and the 95 kDa forms of NHE1 in the total and unbound fractions. It was not possible to efficiently elute biotin labeled proteins bound to immobilized streptavidin resin for direct measurement of extracellular NHE1 protein.

14. Analysis of protein expression levels

Protein concentrations were measured three times using a BioRad DCTM protein assay kit. The NHE1 bands were detected by western blotting as described previously (in the SDS-PAGE and immunoblotting section). Quantification was done using Image J software.

15. Statistics

All activity assays and surface localization results were repeated at least 6-8 times. Protein expression levels were determined 3-4 times. Statistical significance was calculated using Mann-Whitney-Wilcoxon test (170).

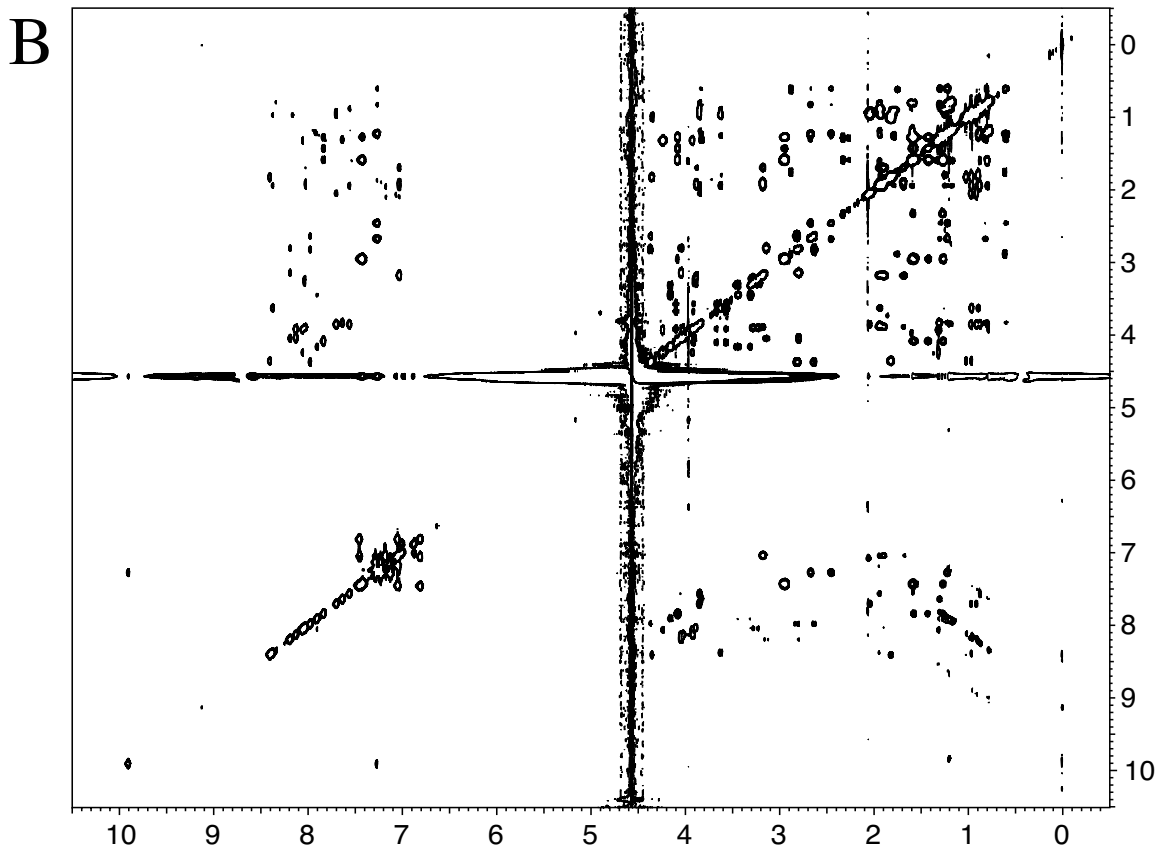
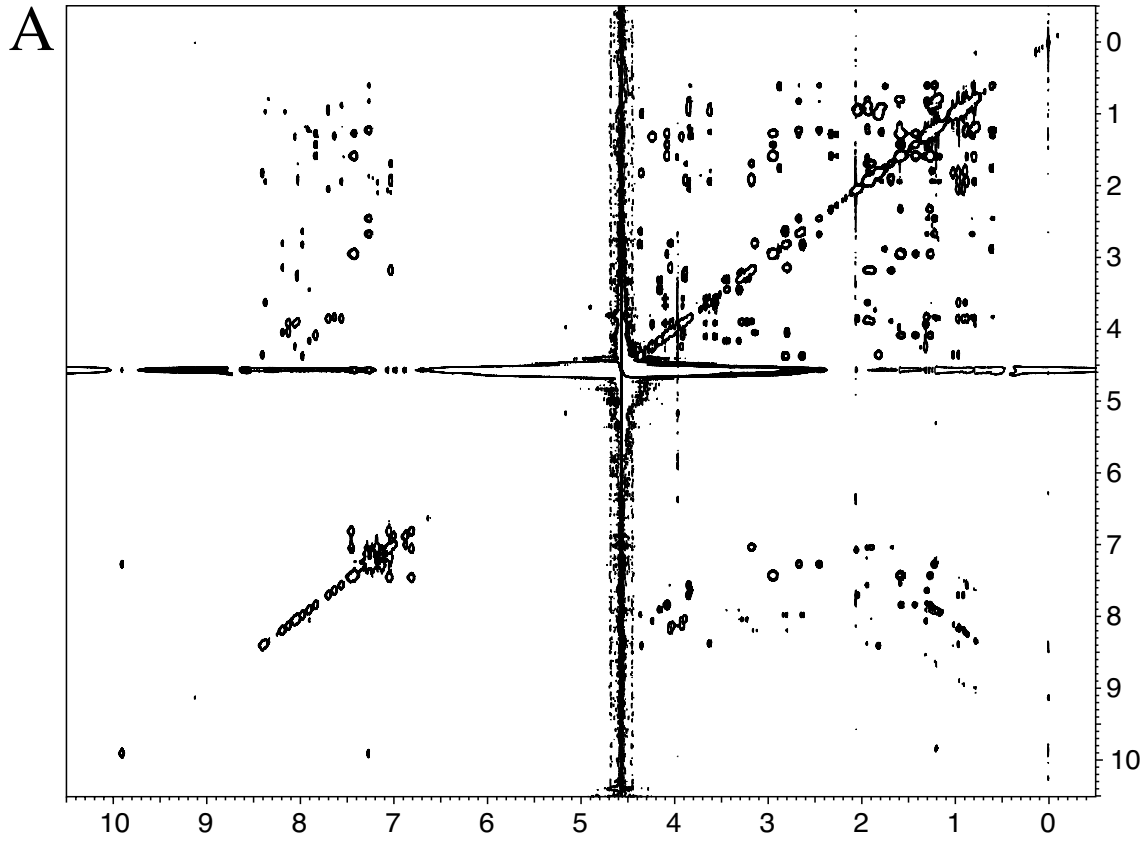


Figure 5. Spectra of IL5 in SDS solution. **A.** NOESY Spectrum of IL5 peptide 5 mM. The spectrum was recorded at 700 MHz with a mixing time of 150 ms at 40°C. **B.** TOCSY Spectrum of IL5 peptide 5 mM. The spectrum was recorded at 700 MHz with a mixing time of 65 ms at 40°C.

Spectra generated with the help from Dr. Ryan McKay

16. NMR spectroscopy in deuterated DMSO (*All NMR spectra was ran and analyzed with the help from Dr. Brian Sykes*)

For the initial sample, 2.8 mg of IL5 peptide was dissolved in 600 μ L deuterated DMSO to a final concentration of \sim 2.8 mM. NMR spectra were acquired on an Agilent VNMRs 700 MHz spectrometer, equipped with an HCN cold-probe and Z-axis pulsed field gradients. For side chain chemical shift assignments, the following experiments were performed 2D $^1\text{H}, ^1\text{H}$ -TOCSY, and a 2D $^1\text{H}, ^1\text{H}$ -NOESY. NMR restraints used for 3D structure generation were automatically obtained from CYANA 2.1(171) using the 2D $^1\text{H}, ^1\text{H}$ -TOCSY assignments and 2D $^1\text{H}, ^1\text{H}$ -NOESY 'cleaned' peak list. Cleaned means that the raw NOE peaks were filtered for non-interatomic diagonals and artifacts. Only the highest confidence peaks were submitted to CYANA 2.1 for auto NOE assignment. Data were processed with NMRPipe (172) and analyzed with NMRView (173).

17. NMR spectroscopy in deuterated SDS (*All NMR spectra was ran and analyzed with the help from Dr. Ryan McKay*)

The IL5 peptide (pH \sim 6, uncorrected for deuterium isotope effect) was dissolved in 540 μ L of H_2O with 58.5 μ L of D_2O (90:10 ratio) with a final SDS concentration of 440 mM. The 10% D_2O as was used as an internal NMR lock solvent. Final peptide concentration was \sim 5 mM. SDS was planned to be at least 80 fold higher in concentration than the peptide to ensure proper micelle formation, and to limit the number of peptide molecules per micelle. We added an extra 10%

SDS to insure this ratio and therefore came to a final concentration of 440 mM for SDS.

NMR spectra of the SDS/micelle peptide sample (see Figure 5) were acquired on a Varian Inova 600 MHz spectrometer, equipped with an HCN triple resonance probe with Z-axis pulsed field gradients. For side chain chemical shift assignments, the following experiments were performed 2D $^1\text{H}, ^1\text{H}$ -TOCSY, 2D $^1\text{H}, ^1\text{H}$ -NOESY, and 2D $^1\text{H}, ^{13}\text{C}$ -HSQC used to confirm assignments in ambiguous regions. NMR restraints used for 3D structure generation were automatically obtained from CYANA 2.1 using the 2D $^1\text{H}, ^1\text{H}$ -TOCSY assignments and 2D $^1\text{H}, ^1\text{H}$ -NOESY 'cleaned' peak list. The raw NOE peaks were filtered for diagonals and artifacts. Only the highest confidence peaks were submitted for auto NOE assignment. Data were processed with NMRPipe (172) and analyzed with NMRView (174).

Stage	1	2	3	4	5	6	7	Refine
Peaks:								
selected	547	547	547	547	547	547	547	
assigned	422	430	423	424	414	413	414	
unassigned	125	117	124	123	133	134	133	
with diagonal assignment	0	0	0	0	0	0	0	
Cross peaks:								
with off-diagonal assignment	422	430	423	424	414	413	414	
with unique assignment	147	235	267	284	293	305	301	
with short-range assignment $ i-j \leq 1$	348	339	332	328	325	320	318	
with medium-range assignment $1 < i-j < 5$	74	85	86	90	83	87	90	
with long-range assignment $ i-j \geq 5$	0	6	5	6	6	6	6	
Upper distance limits:								
Total	241	223	227	217	211	208	255	255
short-range, $ i-j \leq 1$	182	154	158	144	145	140	165	165
medium-range, $1 < i-j < 5$	59	69	66	69	63	65	85	85
long-range, $ i-j \geq 5$	0	0	3	4	3	3	5	5
Average assignments/constraint	3.47	2.3	1.72	1.61	1.51	1.47	1	1
Average target function value	3.94	2.69	6.25	1.14	0.32	0.19	0.39	0.3
RMSD (Residues 1-13):								
Average backbone RMSD to mean	1.06	0.56	0.3	0.41	0.39	0.5	0.28	0.24
Average heavy atom RMSD to mean	1.69	0.87	0.54	0.65	0.61	0.68	0.46	0.37

Table 2. CYANA 2.1 statistics for IL5 peptide structural calculations.

Table generated with the help from Kaitlyn Towle

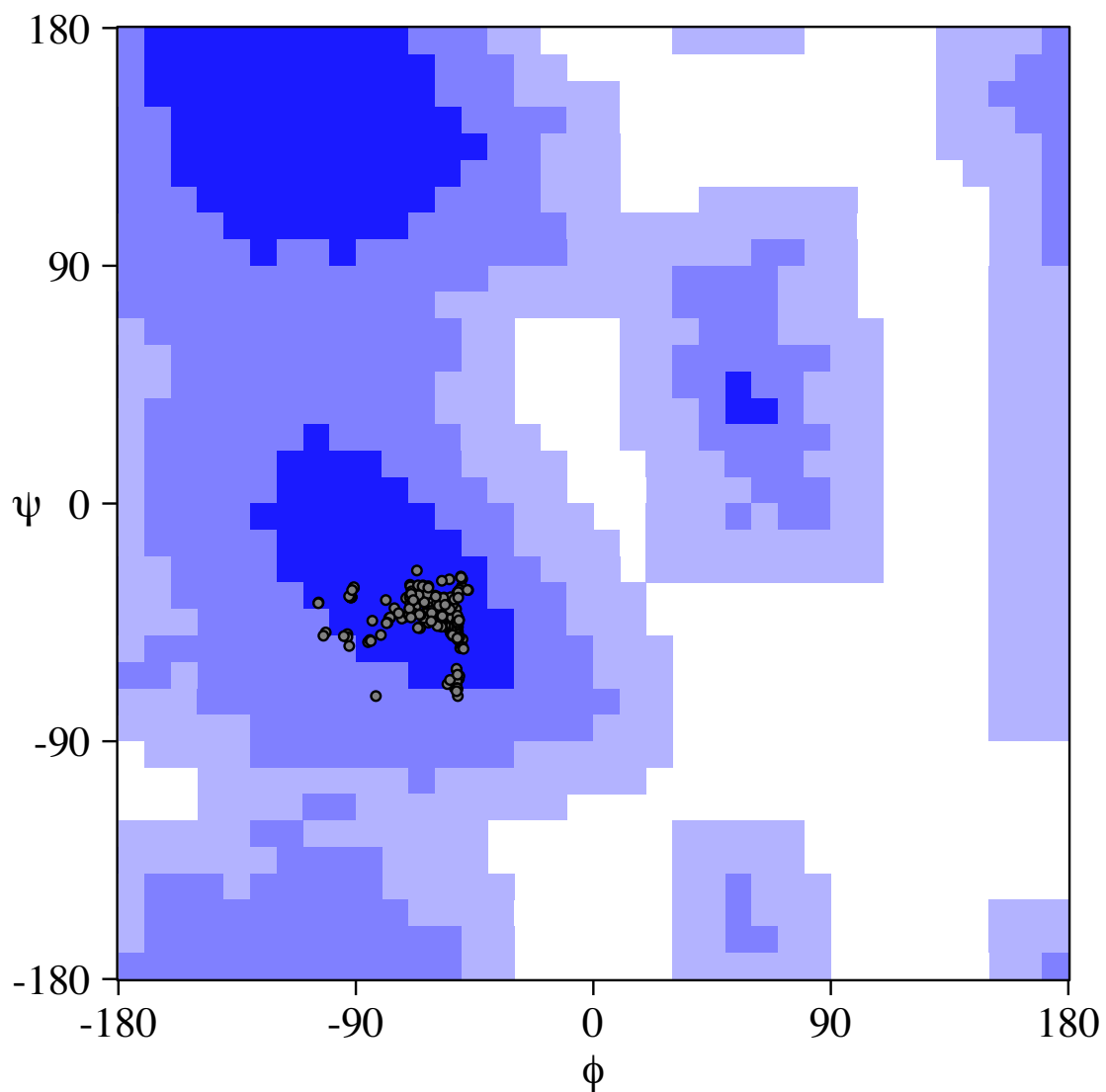


Figure 6. Ramachandran plot for IL5 protein. 95.9% in most favored region, 4.1% in additionally allowed regions, 0.0% in generously allowed regions and 0.0% in disallowed regions.

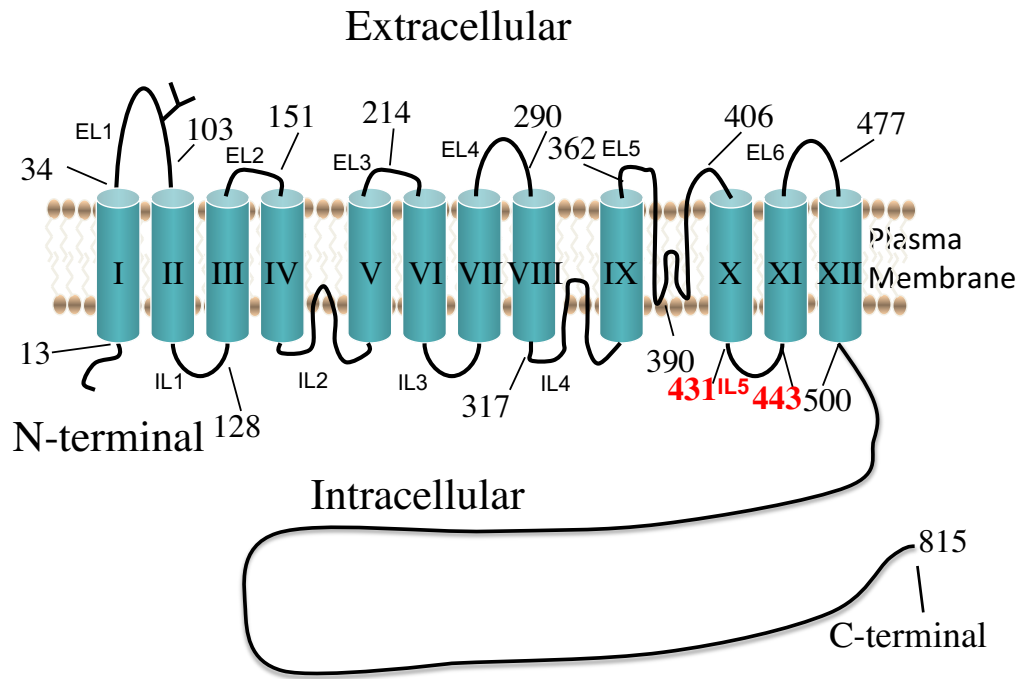
Plot generated with the help from Dr. Ryan McKay

18. Structure calculations

Structures of IL5 peptide was calculated with CYANA 2.1, using nuclear Overhauser effect (NOE) restraints obtained from the 2D-NOESY experiments. Peaks were manually picked and chemical shifts assigned from 1D- ^1H , 2D- ^1H , ^1H -TOCSY, NOESY, and ^1H , ^{13}C -HSQC based experiments. NOEs were selected and calibrated within CYANA according to cross-peak intensities. After seven rounds of calculation (10,000 steps per round), a total of 547 NOE restraints were unambiguously assigned and from these, 414 NOEs were used during the final round of structural calculation (see Table 2). One hundred structures were generated per round, and the 20 lowest energy conformations without NOE violations >0.3 Å or residues in the disallowed region of the Ramachandran plot (see Figure 6), were chosen as representative of the solution structure of IL5 peptide. Structures for this publication were generated using PyMOL Molecular Graphics System, Version 1.8 Schrödinger, LLC (175). including electrostatic surface calculations computed with the optional Adaptive Poisson-Boltzmann Solver (APBS) tools [ref <http://www.poissonboltzmann.org>].

Chapter III Results

A



B

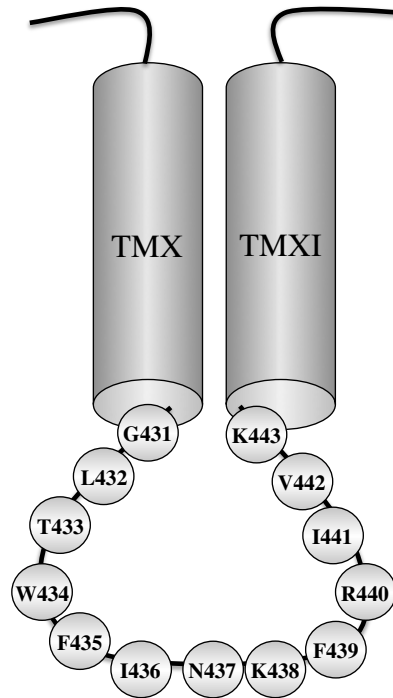


Figure 7. A. A topological model of the IL5 of the transmembrane domain of the NHE1 isoform of the Na^+/H^+ exchanger. **B.** An enlarged diagram of the IL5 peptide.

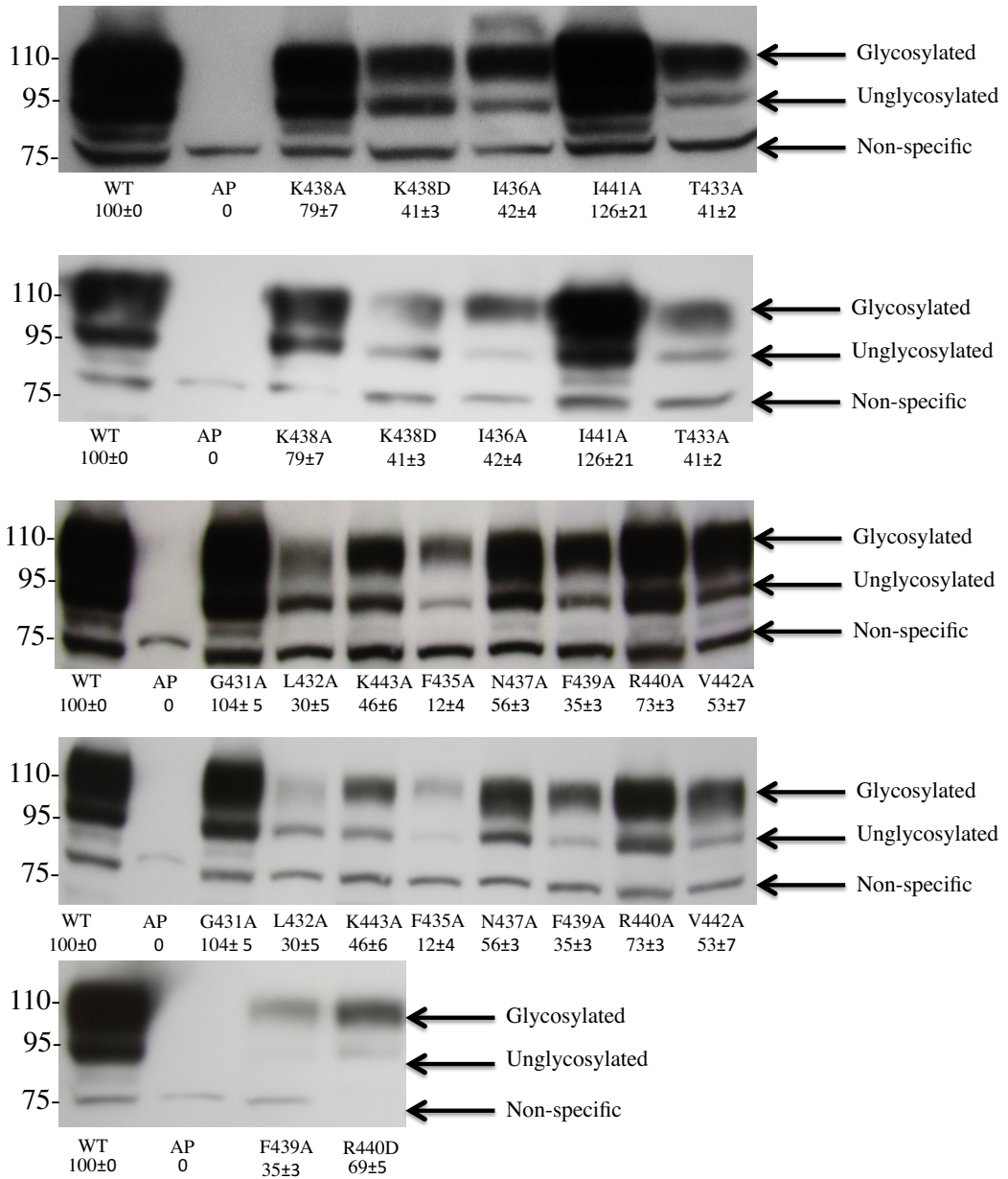
Human	431	GLTWF INKFRIVK	444	[44]
Porcine	431	GLTWF INKFRIVK	444	[46]
Bovine	431	GLTWF INKFRIVK	444	(#Q28036)
Rabbit	431	GLTWF INKFRIVK	444	[45]
Coturnix	423	VLTFW INKFRIVK	436	(ABJ88911)
Amphiuma	439	GLTSV INKFRIVK	452	[47]
Xenopus	409	GLTWF INKFRIVK	422	[49]
Ornithorhynchus	423	GLTFI INKFRIVK	436	[50]
Drosophila	529	LLSAL ANRERLHK	542	(NM 134647)
		*: . *:***: *		

Figure 8. Alignment of amino acid sequence of IL5 and surrounding region of various NHE1 proteins. The alignment was made manually. The shaded region (*) is where the amino acids are conserved amongst those species. The last column indicates Genbank accession numbers in the program BLAST.

1. Characterization of IL5 mutant proteins

A model of IL5 peptide with amino acids (G431-K443) is shown in Figure 7. The IL5 peptide contains several acidic residues and a mixture of hydrophilic and hydrophobic residues. We subjected IL5 to both site-specific mutagenesis, and alanine scanning mutagenesis to investigate the contribution and function of each residue. For alanine scanning mutagenesis, all residues of IL5 were sequentially changed to non-polar and hydrophobic alanine in the WT NHE1 protein. Alanine is a hydrophobic, helix forming amino acid that is relatively small non-intrusive amino acid (176). In addition to alanine scanning mutagenesis, the two polar and positively charged residues Arg440 and Lys438 were mutated into polar and negatively charged residues, R440D and K438D. Figure 8 shows the alignment of amino acid sequence of IL5 and surrounding region of various NHE1 proteins. The shaded region indicates the amino acids are conserved amongst those species.

A



B

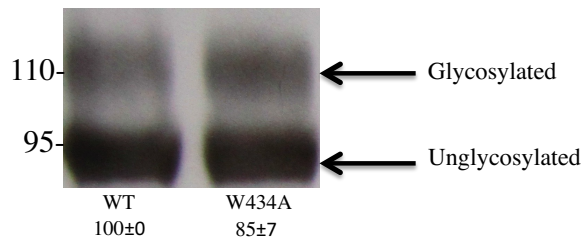


Figure 9. A. Western blot of whole cell lysates of stable cell lines expressing Na⁺/H⁺ exchanger IL5 mutants G431A to T433A, F435A to K443A, K438D and R440D. Mutations are as indicated. Upper panel longer film exposure and lower panel shorter film exposure. **B.** Western blot of whole cell lysates of transiently transfected expressing Na⁺/H⁺ exchanger IL5 mutant W434A. 100 µg of total protein was loaded in each lane. Numbers below the lanes indicate the amount of NHE1 protein relative to wild type NHE. Mean values (n=3) were obtained from densitometric scans of both the 110-kDa (upper) and 95-kDa (lower) bands. AP-1 cells refer to AP-1 cells mock transfected. WT refers to cells stably (**A**) or transiently (**B**) expressing wild type Na⁺/H⁺ exchanger protein.

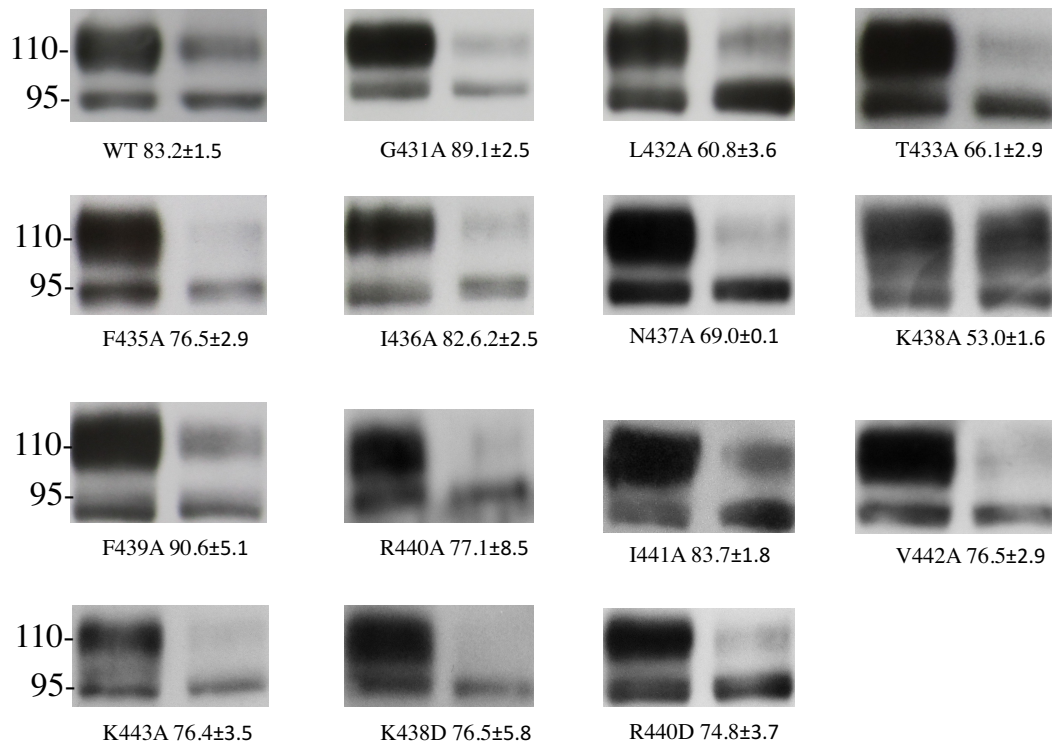
1.1. Expression levels of IL5 protein mutants of NHE1

We initially examined the expression levels of mutant NHE1 proteins expressed in AP-1 cells. Figure 9 shows these results. Expression levels were determined by western blotting with antibody against the HA tag on the Na⁺/H⁺ exchanger protein. Two clones of each mutant cell line and samples were analyzed in triplicate in order to lower the standard error. Figure 9 indicates that all of the mutant proteins were expressed. We were able to obtain stable cell lines for all of the mutant proteins (see Figure 9A) except for W434A protein (see Figure 9B). For W434A protein, despite screening over 100 colonies, we were unable to obtain a stable cell line for unknown reasons. We therefore characterized this protein using transient transfections. Figure 9B shows that the W434A mutant protein expresses with transient transfection. As published earlier (167), NHE1 was expressed as both a fully glycosylated protein around 105-110 KDa and a partial or de-glycosylated protein at around 85-95 KDa. These two immunoreactive bands (see Figure 9) were present in all stable cell lines and transiently transfected cells. AP-1 cells serves as a negative control because those cells do not contain NHE1 hence the absence of these two major bands.

The expression levels of mutant proteins in relation to the WT protein for both stable and transient transfections are shown in Figure 9A and Figure 9B, respectively. Expression levels of several of the mutant proteins were reduced. Most notably, the expression level of the F435A protein was about 10% of the level of the WT protein. The mutants L432A, T433A, I436A, F439A, K443A, K438D also had reduced expression that was between 30% and 50% of WT. The mutants

N437A and V442A had reduced expression that was about half the WT protein. The remaining mutant proteins, K438A, R440A, and R440D, had some slight decreases in expression compared to the WT protein. However, both G431A and I441A had expression levels that were greater than the WT protein. For the transiently transfected W434A protein, there was only a slight decrease in expression compared to WT transiently transfected protein (see Figure 9B).

A



B

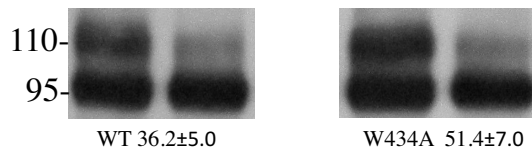


Figure 10. A. Stable cell line and **B.** transiently transfected in AP-1 cells. Surface localization of NHE1 in AP-1 cells expressing control and IL5 mutants. Equal amounts of total cell lysate (left lane) and unbound intracellular lysate (right lane) were examined by western blotting with anti-HA antibody to identify NHE1 protein. WT are cells lines stably expressing wild type NHE1. The percent of the total NHE1 protein found on the plasma membrane is indicated for each mutant. The mean \pm S.E. $n \geq 4$ determinations. Results indicate the percentage of protein that is targeted

to the plasma membrane. Autoradiography exposure times were increased for mutants expressing lower levels of protein.

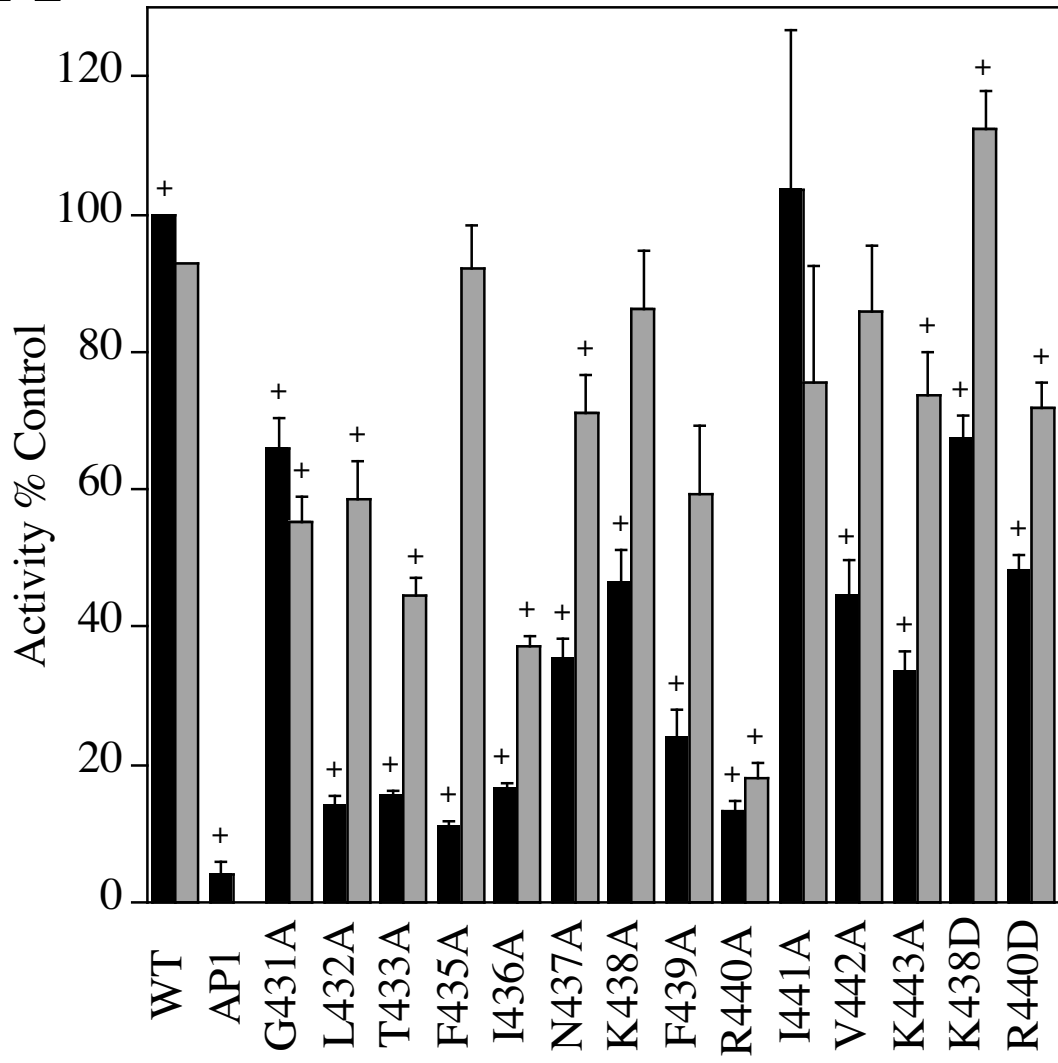
1.2. Surface targeting of IL5 mutant proteins of NHE1

The endoplasmic reticulum contains a variety of enzymes that are necessary for the assembly of membrane proteins. Once a membrane protein is translated, it travels in membrane bound vesicles to the golgi apparatus and eventually to the designated plasma membrane. In order for NHE1 protein to perform its function, it must be targeted to the plasma membrane; if it fails to do so then NHE1 protein is retained in the intracellular compartment and cannot extrude protons out of the cell. Previous studies have shown that certain mutations in NHE1 may result in intracellular retention (77,177). Therefore we examined the surface targeting of the mutant proteins. Cell surface biotinylation experiments were performed (see Figure 10). Briefly, equal amounts of the cell lysates, “Total” and “Unbound” were made. Total protein represents total NHE1 protein in the cell. The unbound fraction is the NHE1 protein in the intracellular compartment after treatment of lysates with streptavidin agarose (for detailed protocol please refer to materials and method section). The difference between “Total” and “Unbound” would be the amount of protein targeted to the plasma membrane surface. The NHE1 protein bands were determined by SDS-PAGE and western blotting with antibody against the HA tag on the Na⁺/H⁺ exchanger protein. Once the blots were visualized by ECL and exposed to a film, the bands were compared and quantified using ImageJ 1.35 software (111).

Most of the wild type, mutant proteins of the stable cell lines and transiently transfected cells (W434A) were well targeted to the cell surface (70-90%, see Figure 10B). However, the K438A protein averaged only about 50% targeting to the cell

surface and L432A, T433A, and N437A proteins were slightly lower (see Figure 10A).

A



B

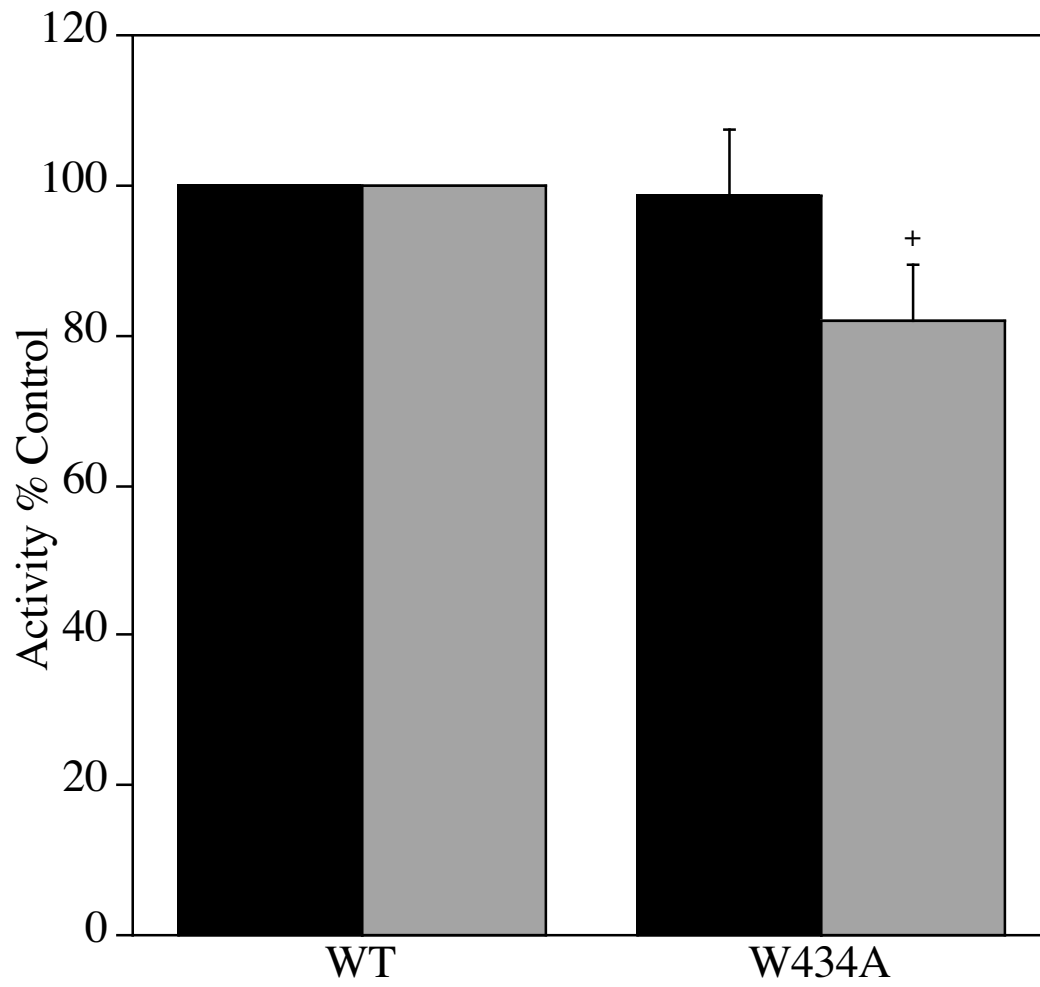


Figure 11 A. Stable cell line and **B.** transiently transfected WT NHE1 and W434A mutant protein. Summary of rate of recovery of AP-1 cells after an acute acid load. The mean activity of WT stably transfected with NHE1 was 0.021 Δ pH/min, and this value was set to 100% and other activities are a percent of those of WT. Values are the mean \pm 8-10 determinations. Results are shown for mean activity of both uncorrected (black) and normalized for levels of surface processing and expression levels (gray). + indicates uncorrected IL5 mutant activities that are significantly lower than that of WT NHE1 at $P < 0.05$.

1.3. Activity assay of IL5 mutant protein containing cells

The Na⁺/H⁺ transport activity of WT and mutant NHE1 proteins was measured by a spectrofluorometric method with the fluorescent dye, BCECF-AM (for detailed protocol please refer to the materials and method section). Figure 4 shows a sample of an activity trace of NHE1 activity. The rate of recovery (activity) is measured and is plotted in a graph for both stable (see Figure 11A) and transient transfections (see Figure 11B). The activity of the IL5 mutant proteins with and without corrections of levels of expression and surface targeting is shown in Figure 11. The uncorrected activity of the IL5 mutant proteins (shaded in black) and normalized activity with expression and mature NHE1 protein surface localization levels (shaded in grey). AP-1 cells had less than 5% of the WT protein. Only I441A had activity comparable to WT. The mutant proteins G431A, K438A, V442A, K438D and R440D had activity between 40 and 70% of WT protein. The mutant proteins N437A, F439A and K443 had activity 25 to 40% of WT protein, and the mutant proteins L432A, T433A, F435A, I436A, R440A had activity only slightly greater than background levels, approximately 10-20% that of WT protein (see Figure 11A). The transiently transfected mutant protein W434A had activity comparable to the transiently transfected WT NHE1 (see Figure 11B).

To determine the level of NHE1 activity that is independent of protein expression level and surface targeting we corrected for surface processing and expression levels (see Figure 11A). It appeared to be that the activity level of mutants F435A, N437A, K438A, I441A, V442A, K443A and R440D were comparable with the WT protein after correction. The mutants G431A, L432A, T433A and

F439A had an activity level that is between 50% to 70% of the WT protein. There were two mutants I436A and R440A that had an activity level of 40% and 20% respectively. Lastly, the K438D protein had an activity level that was greater than the WT protein after correction. The transiently transfected mutant protein W434A had activity comparable to the transiently transfected WT NHE1 (see Figure 11B).

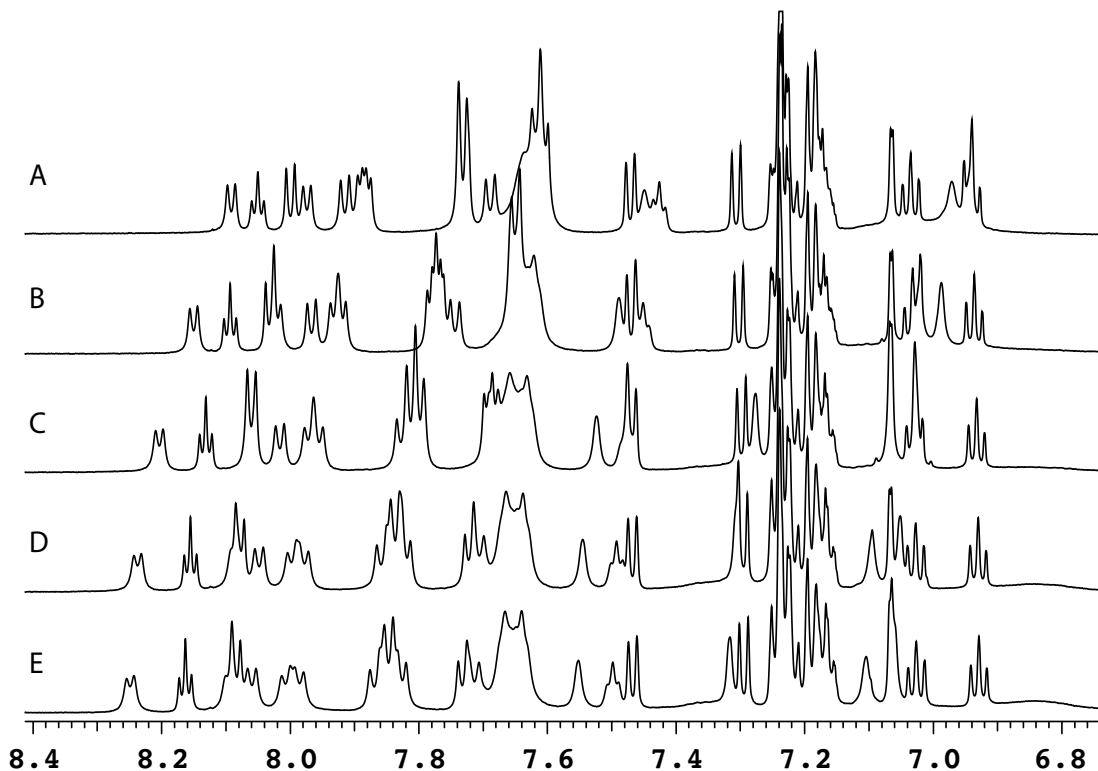


Figure 12. Temperature titration of ~ 2.8 mM of DMSO. Temperature titration of the DMSO solvated sample. Inova 600 MHz VNMRs spectrometer showing 18, 20, 27, 35 and 45°C (E to A) ^1H -1D spectra. Spectra were collected with a 8012.0 Hz sweep width, with 40000 complex points, and 16 scans per FID. Note the collapse of chemical shift dispersion as the temperature increases. Based on this result, 18.1°C (i.e. just above DMSO freezing) was selected as the optimal temperature for final 2D-NOESY data acquisition and assignments.

Spectra generated with the help from Dr. Ryan McKay

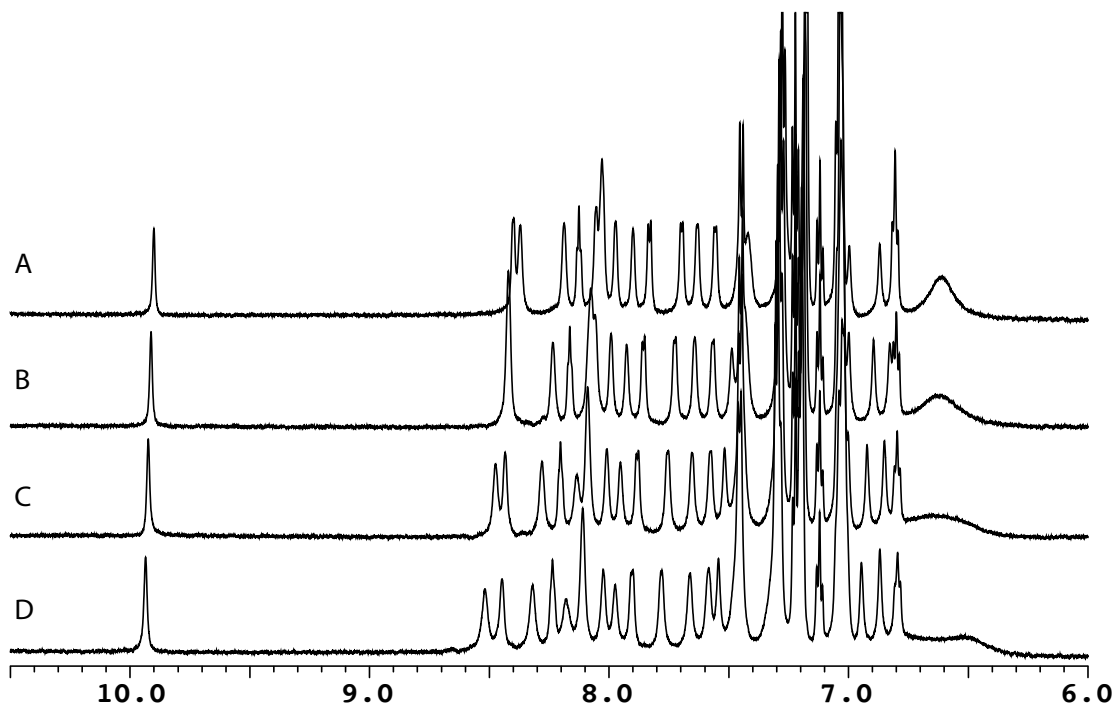


Figure 13. Temperature titration of 440 mM of SDS. Temperature titration of the SDS sample. Inova 600 MHz VNMRs spectrometer showing 27°C, 30°C, 35°C and 40°C (D to A) 1H-1D spectra. Spectra were collected with a 7183.9 Hz sweep width, with 14368 complex points, and 4 scans per FID. Note the collapse of chemical shift dispersion as the temperature increases. Based on this result, 27.0°C was selected as the optimal temperature for final 2D-NOESY data acquisition and assignments.

Spectra generated with the help from Dr. Ryan Mckay

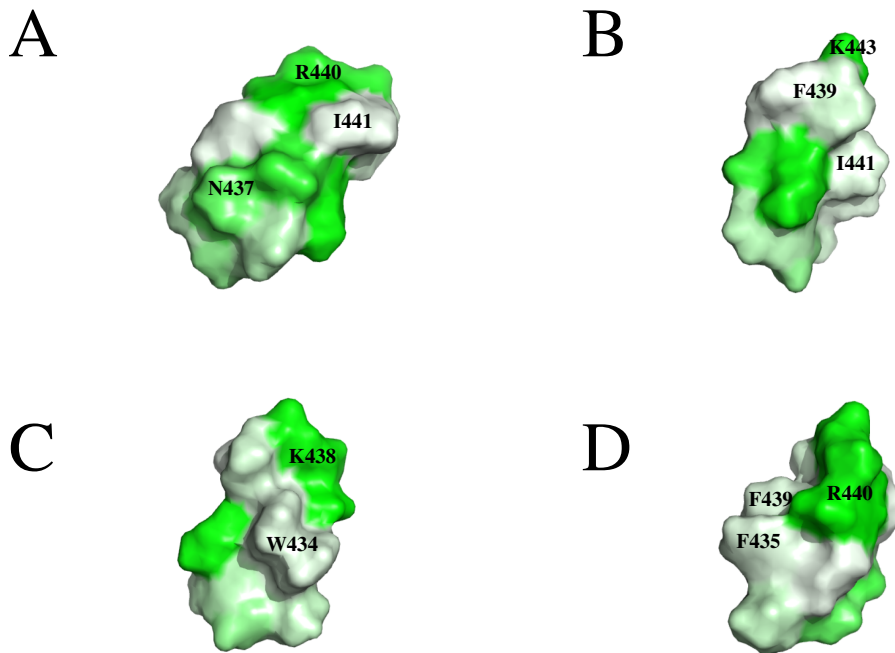


Figure 14. IL5 in different orientations. Representative hydrophobic surface structure of IL5 peptide in different orientations created with PyMOL. Green indicates hydrophilic residues and white indicates hydrophobic residues. The intensity of the green or white colors indicates the degree of hydrophobicity or hydrophilicity of each amino acid residue respectively. A. Front view, B. Rotated 90°, C. Rotated 180° D. Rotated 270°. For all figures N-terminal in the bottom left corner and C-terminal in the top right.

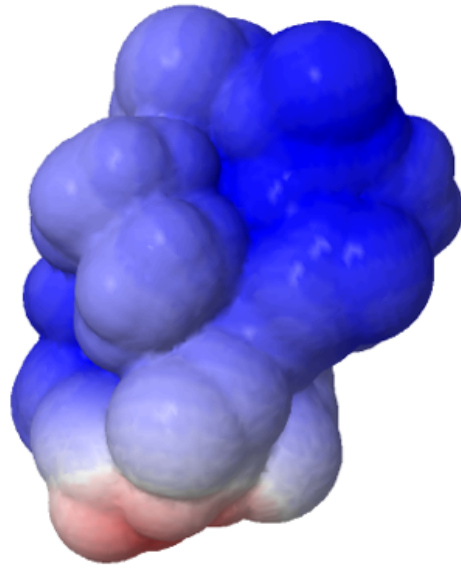


Figure 15. Electrostatic potential maps of IL5 peptide. Cationic regions are blue and anionic regions are red. N-terminal in the bottom left corner and C-terminal in the top right

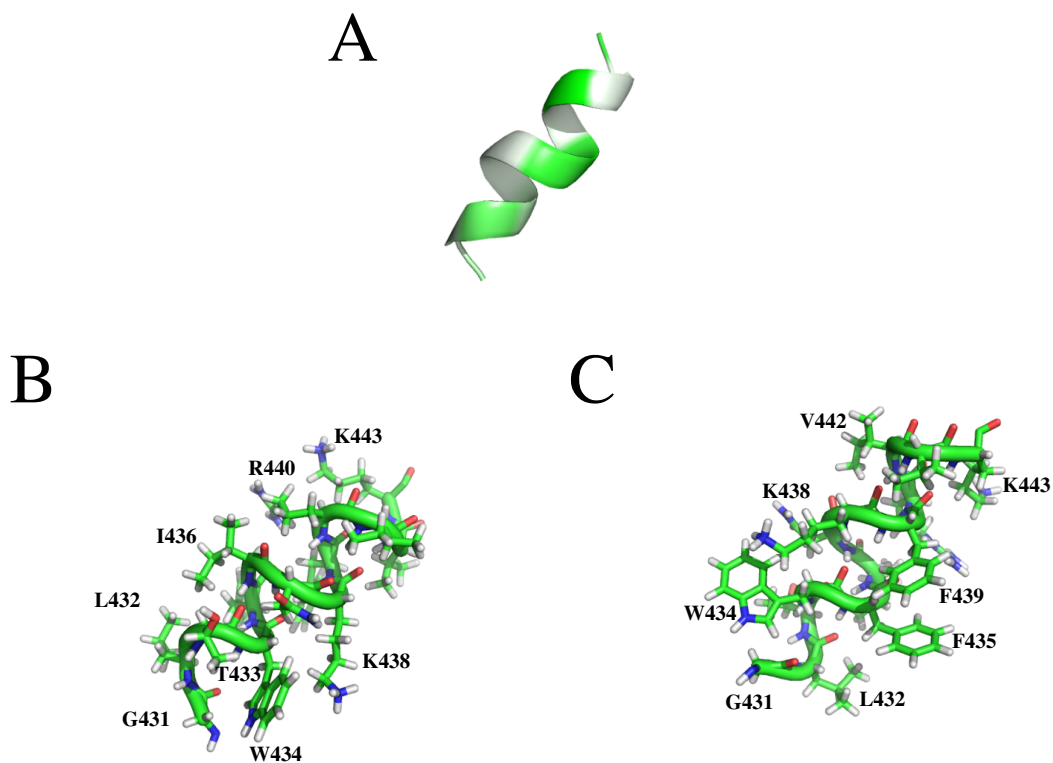


Figure 16. Structural characteristics of IL5. **A.** Ribbon diagram depicting the IL5 peptide. Hydrophobic sidechains are drawn as sticks. **B.** Structure diagram depicting the IL5 peptide showing Lys-Trp-Ser-stick where Lys438 getting close to Trp434. **C.** Sticks-ribbon-ringlock diagram depicting the IL5 peptide. For all figures N-terminal in the bottom left corner and C-terminal in the top right

2. Structural characterization of IL5 protein

Initially we attempted to use DMSO as a solvent hypothesizing that the peptide would utilize the hydrophobic environment as a membrane mimetic. Preliminary 1D-¹H NMR spectra in deuterated DMSO were acquired at 18, 20, 27, 35 and 45° (see Figure 12). Spectra acquired at 18° showed the best resolution of peaks in the downfield amide region, and therefore all subsequent 2D spectra were obtained at this temperature. As shown in Figure 12, temperatures above 18° showed more peak overlap especially in the region from ~7.0 to 7.4 ppm. The chemical shift assignment from the 2D ¹H,¹H-TOCSY and 2D ¹H,¹H-NOESY contained cross-peak ambiguities due to this overlap. Despite this added complexity, backbone and side-chain assignments were completed and a preliminary structure generated. The CYANA 2.1 results for the peptide in DMSO appeared to be completely unstructured.

To determine whether the IL5 loop has a defined structure, a different solvent system was used. We obtained 1D-¹H NMR spectra at 40°, 35°, 30° and 27° with IL5 peptide dissolved in 440 mM SDS buffer solution (10% D₂O NMR lock solvent and 90% H₂O) in order to determine the extent of structure throughout the molecule. As shown in Figure 13, spectra obtained at temperatures above 27° were slightly less resolved, but fine couplings evident, and therefore 40° was chosen for the acquisition of 2D spectra for analysis. Final temperature selection was a combination of resolution, and line-width considerations. IL5 peptide in SDS buffer solution was fully assigned (see previous section), and NOE cross-peaks picked carefully based on absorptive shape, and presence/absence of artefacts in those

regions (*e.g.* T₁ noise streaks or multiple diagonals would have disqualified peak selection). Structures generated using CYANA 2.1 (see Table 2) indicated that IL5 peptide is strongly alpha helical. When torsion angles were evaluated (see Ramachandran plot Figure 6), we see no residues are in the disallowed regions. The final representative structure in two different orientations (~90° rotation along the helical backbone) are shown in Figure 16. Interestingly it appears that Trp434 is extremely close to Lys 438, with the side-chain of K438 pointed into the aromatic system of W434. Electrostatic surfaces are displayed in Figure 15, and we can see from the figures that residue 10 (R440) seems to form physical and electrostatic pockets. Figure 14 shows the hydrophilic and hydrophobic regions at different orientations starting from A. front view, B. 90 degree of rotation, C. 180 degree of rotation, and D. 270 degree of rotation.

Chapter IV Discussion

1. Critical residues of IL5

In this study we examined the structure and function of IL5 of the NHE1 isoform of the Na⁺/H⁺ exchanger. Examination of the residues critical in function revealed that the IL5 loop is greatly sensitive to mutation. When compared with the unaltered NHE1 activity, we found that mutation to alanine resulted in 11 mutant proteins (*i.e.* G431A, L432A, T433A, F435A I436A, N437A, K438A, F439A, R440A, V442A, K443A) in which the activity was significantly reduced. The IL5 loop is therefore very sensitive to alteration of amino acid side chains. The cause of the loss in activity could either be due to defective expression, or a direct effect of the mutation on the protein. In the mutants: G431A, L432A, T433A, F435A, I436A, N437A, K438A, F439A, R440A, V442A, K443A, K438D, and R440D, correction for the amount of protein or targeting of the protein showed that the protein was functional, or nearly so (see Figure 11). In the mutants W434A and I441A, correction for protein levels or targeting did not result in an activity comparable to controls therefore indicating that the mutation caused a defective NHE1 protein. This strongly suggests that the side chains of these particular amino acids are critical in the function (and possibly in tertiary structure) of these proteins. Other mutant proteins with defective activity appear to be mostly or partially affecting targeting or surface processing of the protein.

In addition, we also made two other mutations. Arg440 and Lys438 were independently mutated to aspartic acid in order to reverse the charge of these two amino acids. We found a significant decrease in activity in the K438D mutant,

however, it was found that this reduction was due to effects on expression and surface targeting.

The activity of the R440D mutant was reduced. A previous study (88), examined the effect of R440D mutation on pH dependence on exchanger activity. They demonstrated that this mutation caused an acidic shift in the pH dependence of activity. It is known that ATP depletion decreases NHE1 pH internal sensitivity. In their experiments, ATP depletion did not change the NHE1 activity of cells expressing R440D mutation. In our hands, the R440D mutation caused a decrease in activity of the NHE1 when measured at a strongly acidic pH_i ($pH_i < 7$). This was independent of the effects on surface expression and protein targeting. It was notable that the R440A mutation caused a larger effect than the R440D mutation, indicating that while the arginine residue was important, a negative charge was not necessary for inhibiting activity. Along these lines, it was previously shown that a R440C mutant protein is also defective compared to the WT protein, shifting the pH dependence to an acidic side and reducing the maximum activity (178). It is therefore clear that the R440 amino acid is sensitive to mutation, with varying effects depending on the side chain's chemistry. It was surprising that mutation to alanine had the greatest effects, rather than reversing the charge. It may be that the steric bulkiness of the side chain is important for the structure of the protein, and/or the hydrophobic nature may result in differential binding or final positioning of the peptide. Aggregation/non-specific binding may also be playing a role, which will require further study to describe.

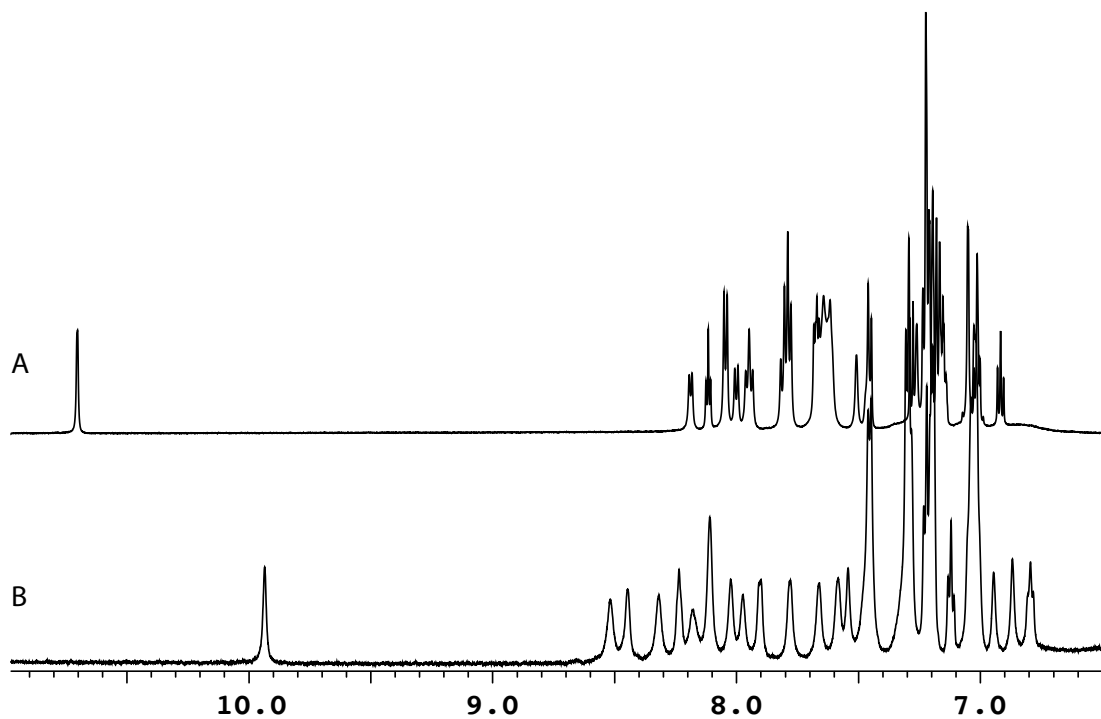


Figure 17. 1D Spectra of IL5 in ~2.8 mM of DMSO and 440mM of SDS solution. A comparison of IL5 peptide in DMSO solution and SDS solution at their optimal temperature. A. DMSO 18.1°C (top) B. SDS 27°C (bottom).

Spectra generated with the help from Dr. Ryan McKay

2. Analysis of IL5 structure and function

High-resolution NMR analysis of the IL5 peptide indicated a mostly alpha helical structure when in the presence of SDS micelles. Initially we attempted to determine the structure of IL5 peptide when dissolved in DMSO. DMSO has an intermediate dielectric constant of approximately ~ 46 (179) and is therefore similar to a membrane interface (180). It was hoped that DMSO would result in a reasonable mimetic of the environment experienced by the peptide loop. In previous studies, Katragadda *et al.* (181) showed that NMR structures of isolated loops from bacteriorhodopsin in DMSO adopted structures equivalent to the known crystal structure of the protein. Moreover, in the Fliegel lab, two extracellular loops (EL2 and EL4) of NHE1 were elucidated in a DMSO environment (162,182). In the previous findings (162), the EL2 was shown to have inter-helical loops in DMSO solvents. For EL4, likely due to the short length of the peptide, it appears to be that the loop is unstructured and flexible in DMSO (182). IL5 appeared to be completely random coil as indicated by the poorly resolved NH resonances in the peptide, and the lack of any long range or medium range NOE cross-peaks associated with definable secondary structure. A temperature titration was performed for the peptide when dissolved in DMSO Figure 12, and compare to Figure 13 when dissolved in SDS/water. The 1D spectrum of the peptide in DMSO at 18° had the best resolution (Figure 17) and was therefore selected for subsequent data acquisition. Evaluation of the resulting backbone/side-chain chemical shifts and NOE cross-peaks showed no definable secondary structure.

In order to pursue a reliable secondary and/or tertiary structure, IL5 was dissolved in an aqueous solvent with sufficient SDS to exceed the critical micellar concentration. SDS micelles are the most commonly used mimetic for structure determination of peptides associated with biomembrances (183). Dissolving the peptide in the presence of SDS showed no signs of precipitation, and initial spectra did exhibit appropriate broadening as expected when moving from a free peptide into one associated with an SDS micelle. Our first experiments involved a series of temperature titrations (see Figure 13), and after evaluation of the spectra, 40° was chosen for the acquisition of all 2D spectra. The selected temperature gave the best resolution and most narrowest line width providing us the confidence that we had a single, and stable structure for the peptide. Structures were generated automatically using CYANA 2.1 (see Table 2). The assigned chemical shifts were determined as described above, and the carefully trimmed NOE peak list was given to Cyana. Cyana assigned the unambiguous correlations, and then iteratively assigned a weighting function to the ambiguous cross-peaks. Structural restraints were determined by CYANA 2.1 and based on confidence and peak intensities. Seven iterations were performed with assigned correlations being added or eliminated based on previous structure results (*e.g.* ambiguous moved to unambiguous, *etc.*). The final round of structures generated indicated that IL5 peptide was highly alpha helical. Figure 14 shows the resulting structure containing a mixture of both the hydrophilic and hydrophobic regions in a semi-spiral configuration. If the hydrophilic and hydrophobic regions were to have appeared distinctly apart from each other, we could have assumed the peptide resided on the

peripheral surface of the plasma membrane with the other side being fully exposed to the cytoplasm. However, in our case it appears to be a mixture of both regions. Therefore, our empirical results agree with Wakabayashi's model, *i.e.* that IL5 exists as a loop along the surface. Figure 16 shows the structure of the peptide with labelled residues. Unexpectedly, it appeared that the side-chain of Lys 438 positioned very close to the Trp434 aromatic ring system. This must represent some lowest energy configuration but the significance, and the energetic driving force behind this restricted and hindered conformation is not yet understood. Future work must be done in order to reveal the structural purpose of these two residues, as well as the configuration of other residues resembling an aromatic ring (e.g. Trp and Phe).

Chapter V Summary

Summary

In summary, we examined the structure and function of IL5 (residues 431-443) of the NHE1 isoform of the Na⁺/H⁺ exchanger. We found that there are many critical residues in the loop. Eleven out of 13 mutants to alanine had reduced activity. This showed that the IL5 peptide is very sensitive to the alteration of amino acid side chains. We next examined the expression and surface targeting of the mutant proteins. It appeared to be that residues G431-T433, F435-R440A and V442-K443 were functional after the correction for the amount of protein or targeting of the protein. Only mutant proteins, W434A and I441A caused a defective NHE1 protein that was not dependent on changes in expression levels and targeting. In conclusion, this strongly suggested that the side chains of these particular amino acids are critical in the function (and possibly in tertiary structure) of these proteins.

Another interesting finding was the charge reversal experiment that was performed on Arg440 and Lys438. Those amino acids were independently mutated to aspartic acid. The results showed that R440D caused a smaller defect than the R440A mutation. This showed that the charge of this amino acid was insignificant for activity. The nature of the side chain is important, but charge is not the critical determinant of NHE1 function for Arg440.

The structural analysis of IL5 revealed by NMR spectroscopy, showed that in DMSO the IL5 peptide was completely unstructured. To determine whether the IL5 peptide has a defined structure, a different solvent system was used. In the solvent system, SDS, IL5 peptide is shown to be strongly alpha helical. Moreover, the

peptide contained a mixture of both hydrophilic and hydrophobic regions in a spiral configuration. This does not suggest that the protein resided on the peripheral surface of the plasma membrane with the other side being fully exposed to the cytoplasm, rather the findings agreed with Wakabayashi's model that IL5 exists as a loop.

Finally, the structure of the peptide with labelled residues showed that residue Lys438 is very close to the Trp434 residue. This could possibly mean that they both exhibit similar properties. Perhaps these two residues prefer to be exposed or hidden from the hydrophilic solvent. However, further work is necessary to solidify this conclusion.

Chapter VI Future Directions

Future Studies

NHE1 is a protein that is ubiquitously expressed on the plasma membrane in mammals. As an intracellular pH regulator, it is an important protein and worthwhile to be studied. The maintenance of the intracellular pH (pH_i) in cells is vital for survival since a slight alteration in pH_i may lead to pathological consequences. For this reason it is necessary to examine and understand how the NHE1 protein operates in detail. Future studies could investigate each and every binding site of the full length NHE1 protein of inhibitors and regulatory proteins. Additionally powerful electron microscopic tools could be used to examine a high resolution structure of the full length NHE1 protein.

More specifically, for my own project some additional structural work could be done. I strongly suggest that we should perform experiments to test the location of the residues Lys438 and Trp434 and see if they are peripheral to the membrane or are buried inside of the membrane lipid bilayer. That could provide valuable information on their accessibility. Also it is important to examine other close stacking residues in the structure and to determine how they are related to the functional critical residues. For further functional analysis, I would examine the acidic and alkaline shift of all the critical residues that were found in my project examining the effect of their mutation on activity at various intracellular pH's. This would give us more detailed information on how the mutation affected the activity of the NHE1 protein.

References

1. Fliegel, L. (2008) Molecular biology of the myocardial Na⁺/H⁺ exchanger. *J Mol Cell Cardiol* **44**, 228-237
2. Fliegel, L. (2005) The Na⁺/H⁺ exchanger isoform 1. *Int J Biochem Cell Biol* **37**, 33-37
3. Casey, J. R., Grinstein, S., and Orlowski, J. (2010) Sensors and regulators of intracellular pH. *Nat Rev Mol Cell Biol* **11**, 50-61
4. Krogh, A., Larsson, B., von Heijne, G., and Sonnhammer, E. L. (2001) Predicting transmembrane protein topology with a hidden Markov model: application to complete genomes. *J Mol Biol* **305**, 567-580
5. Yildirim, M. A., Goh, K. I., Cusick, M. E., Barabasi, A. L., and Vidal, M. (2007) Drug-target network. *Nature biotechnology* **25**, 1119-1126
6. Brett, C. L., Donowitz, M., and Rao, R. (2005) Evolutionary origins of eukaryotic sodium/proton exchangers. *American journal of physiology* **288**, C223-239
7. Xiang, M., Feng, M., Muend, S., and Rao, R. (2007) A human Na⁺/H⁺ antiporter sharing evolutionary origins with bacterial NhaA may be a candidate gene for essential hypertension. *Proc Natl Acad Sci U S A* **104**, 18677-18681
8. Lee, S. H., Kim, T., Park, E. S., Yang, S., Jeong, D., Choi, Y., and Rho, J. (2008) NHE10, an osteoclast-specific member of the Na⁺/H⁺ exchanger family, regulates osteoclast differentiation and survival [corrected]. *Biochemical and biophysical research communications* **369**, 320-326
9. Orlowski, J., Grinstein, S. (2004) Diversity of the mammalian sodium/proton exchanger SLC9 gene family. *Pflugers Arch* **447**, 549-565
10. Slepko, E., and Fliegel, L. (2002) Structure and function of the NHE1 isoform of the Na⁺/H⁺ exchanger. *Biochem. Cell Biol.* **80**, 499-508
11. Murer, H., Hopfer, U., and Kinne, R. (1976) Sodium/proton antiport in brush-border-membrane vesicles isolated from rat small intestine and kidney. *Biochem J* **154**, 597-604
12. Pouyssegur, J., Chambard, J. C., Franchi, A., Paris, S., and van Obberghen-Schilling, E. (1982) Growth factor activation of an amiloride-sensitive Na⁺/H⁺ exchange system in quiescent fibroblasts: coupling to ribosomal protein S6 phosphorylation. *Proc. Natl. Acad. Sci. USA* **79**, 3935-3939
13. Sardet, C., Franchi, A., and Pouyssegur, J. (1989) Molecular cloning, primary structure, and expression of the human growth factor-activatable Na⁺/H⁺ antiporter. *Cell* **56**, 271-280
14. Kendrew, J. C., Dickerson, R. E., Strandberg, B. E., Hart, R. G., Davies, D. R., Phillips, D. C., and Shore, V. C. (1960) Structure of myoglobin: A three-dimensional Fourier synthesis at 2 Å resolution. *Nature* **185**, 422-427
15. Malo, M. E., and Fliegel, L. (2006) Physiological role and regulation of the Na⁺/H⁺ exchanger. *Canadian journal of physiology and pharmacology* **84**, 1081-1095
16. Amith, S. R., and Fliegel, L. (2013) Regulation of the Na⁺/H⁺ Exchanger (NHE1) in Breast Cancer Metastasis. *Cancer research* **73**, 1259-1264
17. Bell, S. M., Schreiner, C. M., Schultheis, P. J., Miller, M. L., Evans, R. L., Vorhees, C. V., Shull, G. E., and Scott, W. J. (1999) Targeted disruption of the murine

- Nhe1 locus induces ataxia, growth retardation, and seizures. *Am J Physiol* **276**, C788-795
18. Fliegel, L. (2005) The Na⁺/H⁺ exchanger isoform 1. *Int. J. Biochem. Cell Biol.* **37**, 33-37
 19. Malakooti, J., Dahdal, R. Y., Schmidt, L., Layden, T. J., Dudeja, P. K., and Ramaswamy, K. (1999) Molecular cloning, tissue distribution, and functional expression of the human Na⁺/H⁺ exchanger NHE2. *Am. J. Physiol.* **277**, G383-G390.
 20. McSwine, R. L., Musch, M. W., Bookstein, C., Xie, Y., Rao, M., and Chang, E. B. (1998) Regulation of apical membrane Na⁺/H⁺ exchangers NHE2 and NHE3 in intestinal epithelial cell line C2/bbe. *Am J Physiol* **275**, C693-701
 21. Wang, Z., Orłowski, J., and Shull, G. E. (1993) Primary structure and functional expression of a novel gastrointestinal isoform of the rat Na⁺/H⁺ exchanger. *J. Biol. Chem.* **268**, 11925-11928
 22. Ford, P., Rivarola, V., Kierbel, A., Chara, O., Blot-Chabaud, M., Farman, N., Parisi, M., and Capurro, C. (2002) Differential role of Na⁺/H⁺ exchange isoforms NHE-1 and NHE-2 in a rat cortical collecting duct cell line. *The Journal of membrane biology* **190**, 117-125
 23. Schultheis, P. J., Clarke, L.L., Meneton, P., Harline, M., Boivin, G.P., Stemmermann, G., Duffy, J.J., Doetschman, T., Miller, M.L., Shull, G. . (1998) Targeted disruption of the murine Na⁺/H⁺ exchanger isoform 2 gene causes reduced viability of gastric cells and loss of net acid secretion. *J. Clin. Invest.* **101**, 1243-1253
 24. Shugrue, C. A., Obermuller, N., Bachmann, S., Slayman, C. W., and Reilly, R. F. (1999) Molecular cloning of NHE3 from LLC-PK1 cells and localization in pig kidney. *J Am Soc Nephrol* **10**, 1649-1657
 25. He, P., and Yun, C. C. (2010) Mechanisms of the regulation of the intestinal Na⁺/H⁺ exchanger NHE3. *J Biomed Biotechnol* **2010**, 238080
 26. Alexander, R. T., and Grinstein, S. (2009) Tethering, recycling and activation of the epithelial sodium-proton exchanger, NHE3. *J Exp Biol* **212**, 1630-1637
 27. Aronson, P. S. (1996) Role of ion exchangers in mediating NaCl transport in the proximal tubule. *Kidney Int* **49**, 1665-1670
 28. Daniel, H. (2004) Molecular and integrative physiology of intestinal peptide transport. *Annu Rev Physiol* **66**, 361-384
 29. Thwaites, D. T., and Anderson, C. M. (2007) H⁺-coupled nutrient, micronutrient and drug transporters in the mammalian small intestine. *Exp Physiol* **92**, 603-619
 30. Wang, H., Singh, D., and Fliegel, L. (1997) The Na⁺/H⁺ antiporter potentiates growth and retinoic- acid induced differentiation of P19 embryonal carcinoma cells. *J Biol Chem* **272**, 26545-26549
 31. Attaphitaya, S., Park, K., and Melvin, J. E. (1999) Molecular cloning and functional expression of a rat Na⁺/H⁺ exchanger (NHE5) highly expressed in brain. *J Biol Chem* **274**, 4383-4388

32. Orłowski, J., Kandasamy, R. A., and Shull, G. E. (1992) Molecular cloning of putative members of the Na⁺/H⁺ exchanger gene family. *J. Biol. Chem.* **267**, 9331-9339
33. Bookstein, C., Xie, Y., Rabenau, K., Musch, M. W., McSwine, R. L., Rao, M. C., and Chang, E. B. (1997) Tissue distribution of Na⁺/H⁺ exchanger isoforms NHE2 and NHE4 in rat intestine and kidney. *Am J Physiol* **273**, C1496-1505
34. Orłowski, J., and Grinstein, S. (2004) Diversity of the mammalian sodium/proton exchanger SLC9 gene family. *Pflugers Arch* **447**, 549-565
35. Pizzonia, J. H., Biemesderfer, D., Abu-Alfa, A. K., Wu, M. S., Exner, M., Isenring, P., Igarashi, P., and Aronson, P. S. (1998) Immunochemical characterization of Na⁺/H⁺ exchanger isoform NHE4. *Am J Physiol* **275**, F510-517
36. Brant, S. R., Yun, C. H., Donowitz, M., and Tse, C. M. (1995) Cloning, tissue distribution, and functional analysis of the human Na⁺/N⁺ exchanger isoform, NHE3. *Am J Physiol* **269**, C198-206
37. Chambrey, R., Achard, J. M., and Warnock, D. G. (1997) Heterologous expression of rat NHE4: a highly amiloride-resistant Na⁺/H⁺ exchanger isoform. *Am J Physiol* **272**, C90-98
38. Jessen, F., Sjöholm, C., and Hoffmann, E. K. (1986) Identification of the anion exchange protein of Ehrlich cells: a kinetic analysis of the inhibitory effects of 4,4'-diisothiocyano-2,2'-stilbene-disulfonic acid (DIDS) and labeling of membrane proteins with 3H-DIDS. *The Journal of membrane biology* **92**, 195-205
39. Gawenis, L. R., Greeb, J. M., Prasad, V., Grisham, C., Sanford, L. P., Doetschman, T., Andringa, A., Miller, M. L., and Shull, G. E. (2005) Impaired gastric acid secretion in mice with a targeted disruption of the NHE4 Na⁺/H⁺ exchanger. *J Biol Chem* **280**, 12781-12789
40. Baird, N. R., Orłowski, J., Szabo, E. Z., Zaun, H. C., Schultheis, P. J., Menon, A. G., and Shull, G. E. (1999) Molecular cloning, genomic organization, and functional expression of Na⁺/H⁺ exchanger isoform 5 (NHE5) from human brain. *J Biol Chem* **274**, 4377-4382
41. Diering, G. H., Church, J., and Numata, M. (2009) Secretory Carrier Membrane Protein 2 Regulates Cell-surface Targeting of Brain-enriched Na⁺/H⁺ Exchanger NHE5. *J Biol Chem* **284**, 13892-13903
42. Wang, H., Singh, D., and Fliegel, L. (1997) The Na⁺/H⁺ antiporter potentiates growth and retinoic acid-induced differentiation of P19 embryonal carcinoma cells. *J Biol Chem* **272**, 26545-26549
43. Yu, H., Freedman, B. I., Rich, S. S., and Bowden, D. W. (2000) Human Na⁺/H⁺ exchanger genes : identification of polymorphisms by radiation hybrid mapping and analysis of linkage in end-stage renal disease. *Hypertension* **35**, 135-143
44. Spacey, S. D., Szczygielski, B. I., McRory, J. E., Wali, G. M., Wood, N. W., and Snutch, T. P. (2002) Mutation analysis of the sodium/hydrogen exchanger gene (NHE5) in familial paroxysmal kinesigenic dyskinesia. *J Neural Transm (Vienna)* **109**, 1189-1194
45. Nakamura, N., Tanaka, S., Teko, Y., Mitsui, K., and Kanazawa, H. (2005) Four Na⁺/H⁺ exchanger isoforms are distributed to Golgi and post-Golgi

- compartments and are involved in organelle pH regulation. *J Biol Chem* **280**, 1561-1572
46. Kondapalli, K. C., Prasad, H., and Rao, R. (2014) An inside job: how endosomal Na(+)/H(+) exchangers link to autism and neurological disease. *Front Cell Neurosci* **8**, 172
 47. Roxrud, I., Raiborg, C., Gilfillan, G. D., Stromme, P., and Stenmark, H. (2009) Dual degradation mechanisms ensure disposal of NHE6 mutant protein associated with neurological disease. *Exp Cell Res* **315**, 3014-3027
 48. Sardet, C., Franchi, A., and Pouyssegur, J. (1989) Molecular cloning, primary structure, and expression of the human growth factor-activatable Na⁺/H⁺ antiporter. *Cell* **56**, 271-280
 49. Engelman, D. M., Steitz, T. A., and Goldman, A. (1986) Identifying nonpolar transbilayer helices in amino acid sequences of membrane proteins. *Annu Rev Biophys Biophys Chem* **15**, 321-353
 50. Counillon, L., Pouyssegur, J., and Reithmeier, R. A. (1994) The Na⁺/H⁺ exchanger NHE-1 possesses N- and O-linked glycosylation restricted to the first N-terminal extracellular domain. *Biochemistry* **33**, 10463-10469
 51. Wakabayashi, S., Bertrand, B., Shigekawa, M., Fafournoux, P., and Pouyssegur, J. (1994) Growth factor activation and "H(+)-sensing" of the Na⁺/H⁺ exchanger isoform 1 (NHE1). Evidence for an additional mechanism not requiring direct phosphorylation. *J Biol Chem* **269**, 5583-5588
 52. Sardet, C., Counillon, L., Franchi, A., and Pouyssegur, J. (1990) Growth factors induce phosphorylation of the Na⁺/H⁺ antiporter, glycoprotein of 110 kD. *Science* **247**, 723-726
 53. Kyte, J., and Doolittle, R. F. (1982) A simple method for displaying the hydropathic character of a protein. *Journal of molecular biology* **157**, 105-132
 54. Shrode, L. D., Gan, B. S., D'Souza, S. J., Orłowski, J., and Grinstein, S. (1998) Topological analysis of NHE1, the ubiquitous Na⁺/H⁺ exchanger using chymotryptic cleavage. *Am J Physiol* **275**, C431-439
 55. Wakabayashi, S., Pang, T., Su, X., and Shigekawa, M. (2000) A novel topology model of the human Na⁺/H⁺ exchanger isoform 1. *J Biol Chem* **275**, 7942-7949
 56. Landau, M., Herz, K., Padan, E., and Ben-Tal, N. (2007) Model structure of the Na⁺/H⁺ exchanger 1 (NHE1): functional and clinical implications. *J Biol Chem* **282**, 37854-37863
 57. Wakabayashi, S., Pang, T., Su, X., and Shigekawa, M. (2000) A novel topology model of the human Na(+)/H(+) exchanger isoform 1. *J Biol Chem* **275**, 7942-7949
 58. Hunte, C., Screpanti, E., Venturi, M., Rimon, A., Padan, E., and Michel, H. (2005) Structure of a Na⁺/H⁺ antiporter and insights into mechanism of action and regulation by pH. *Nature* **435**, 1197-1202
 59. Haworth, R. S., Frohlich, O., and Fliegel, L. (1993) Multiple carbohydrate moieties on the Na⁺/H⁺ exchanger. *Biochem J* **289** (Pt 3), 637-640
 60. Kemp, G., Young, H., and Fliegel, L. (2008) Structure and function of the human Na⁺/H⁺ exchanger isoform 1. *Channels (Austin)* **2**, 329-336

61. Miyazaki, E., Sakaguchi, M., Wakabayashi, S., Shigekawa, M., and Mihara, K. (2001) NHE6 protein possesses a signal peptide destined for endoplasmic reticulum membrane and localizes in secretory organelles of the cell. *J Biol Chem* **276**, 49221-49227
62. Zizak, M., Cavet, M. E., Bayle, D., Tse, C. M., Hallen, S., Sachs, G., and Donowitz, M. (2000) Na(+)/H(+) exchanger NHE3 has 11 membrane spanning domains and a cleaved signal peptide: topology analysis using in vitro transcription/translation. *Biochemistry* **39**, 8102-8112
63. Liu, Y., Basu, A., Li, X., and Fliegel, L. (2015) Topological analysis of the Na/H exchanger. *Biochim Biophys Acta* **1848**, 2385-2393
64. Henderson, R., and Unwin, P. N. (1975) Three-dimensional model of purple membrane obtained by electron microscopy. *Nature* **257**, 28-32
65. Deisenhofer, J., Epp, O., Miki, K., Huber, R., and Michel, H. (1985) Structure of the Protein Subunits in the Photosynthetic Reaction Center of Rhodospseudomonas-Viridis at 3a Resolution. *Nature* **318**, 618-624
66. Michel, H., Weyer, K. A., Gruenberg, H., Dunger, I., Oesterhelt, D., and Lottspeich, F. (1986) The 'light' and 'medium' subunits of the photosynthetic reaction centre from Rhodospseudomonas viridis: isolation of the genes, nucleotide and amino acid sequence. *The EMBO journal* **5**, 1149-1158
67. Sipos, L., and Vonheijne, G. (1993) Predicting the Topology of Eukaryotic Membrane-Proteins. *European Journal of Biochemistry* **213**, 1333-1340
68. Granseth, E. (2010) Prediction of re-entrant regions and other structural features beyond traditional topology models. *Structural Bioinformatics of Membrane Proteins*, 123-136
69. Screpanti, E., and Hunte, C. (2007) Discontinuous membrane helices in transport proteins and their correlation with function. *Journal of structural biology* **159**, 261-267
70. Moncoq, K., Kemp, G., Li, X., Fliegel, L., and Young, H. S. (2008) Dimeric structure of human Na⁺/H⁺ exchanger isoform 1 overproduced in *Saccharomyces cerevisiae*. *J Biol Chem* **283**, 4145-4154
71. Reddy, T., Li, X., Fliegel, L., Sykes, B. D., and Rainey, J. K. (2010) Correlating structure, dynamics, and function in transmembrane segment VII of the Na⁺/H⁺ exchanger isoform 1. *Biochim Biophys Acta* **1798**, 94-104
72. Fafournoux, P., Noel, J., and Pouyssegur, J. (1994) Evidence that Na⁺/H⁺ exchanger isoforms NHE1 and NHE3 exist as stable dimers in membranes with a high degree of specificity for homodimers. *J Biol Chem* **269**, 2589-2596
73. Hisamitsu, T., Ben Ammar, Y., Nakamura, T. Y., and Wakabayashi, S. (2006) Dimerization is crucial for the function of the Na⁺/H⁺ exchanger NHE1. *Biochemistry* **45**, 13346-13355
74. Hisamitsu, T., Pang, T., Shigekawa, M., and Wakabayashi, S. (2004) Dimeric interaction between the cytoplasmic domains of the Na⁺/H⁺ exchanger NHE1 revealed by symmetrical intermolecular cross-linking and selective co-immunoprecipitation. *Biochemistry* **43**, 11135-11143
75. Wuthrich, K. (1990) Protein structure determination in solution by NMR spectroscopy. *J Biol Chem* **265**, 22059-22062

76. Frueh, D. P., Goodrich, A. C., Mishra, S. H., and Nichols, S. R. (2013) NMR methods for structural studies of large monomeric and multimeric proteins. *Curr Opin Struct Biol* **23**, 734-739
77. Slepkov, E. R., Rainey, J. K., Li, X., Liu, Y., Cheng, F. J., Lindhout, D. A., Sykes, B. D., and Fliegel, L. (2005) Structural and functional characterization of transmembrane segment IV of the NHE1 isoform of the Na⁺/H⁺ exchanger. *J Biol Chem* **280**, 17863-17872
78. Lee, B. L., Li, X., Liu, Y., Sykes, B. D., and Fliegel, L. (2009) Structural and functional analysis of transmembrane XI of the NHE1 isoform of the Na⁺/H⁺ exchanger. *J Biol Chem* **284**, 11546-11556
79. Ding, J., Rainey, J. K., Xu, C., Sykes, B. D., and Fliegel, L. (2006) Structural and functional characterization of transmembrane segment VII of the Na⁺/H⁺ exchanger isoform 1. *J Biol Chem* **281**, 29817-29829
80. Slepkov, E., and Fliegel, L. (2002) Structure and function of the NHE1 isoform of the Na⁺/H⁺ exchanger. *Biochemistry and cell biology = Biochimie et biologie cellulaire* **80**, 499-508
81. Javadpour, M. M., Eilers, M., Groesbeek, M., and Smith, S. O. (1999) Helix packing in polytopic membrane proteins: role of glycine in transmembrane helix association. *Biophys J* **77**, 1609-1618
82. Reddy, T., Ding, J., Li, X., Sykes, B. D., Rainey, J. K., and Fliegel, L. (2008) Structural and functional characterization of transmembrane segment IX of the NHE1 isoform of the Na⁺/H⁺ exchanger. *J Biol Chem* **283**, 22018-22030
83. West, I. C., and Mitchell, P. (1974) Proton/sodium ion antiport in Escherichia coli. *Biochem J* **144**, 87-90
84. Orlov, S. N., Adarichev, V. A., Devlin, A. M., Maximova, N. V., Sun, Y. L., Tremblay, J., Dominiczak, A. F., Postnov, Y. V., and Hamet, P. (2000) Increased Na⁽⁺⁾/H⁽⁺⁾ exchanger isoform 1 activity in spontaneously hypertensive rats: lack of mutations within the coding region of NHE1. *Biochim Biophys Acta* **1500**, 169-180
85. Krulwich, T. A. (1983) Na⁺/H⁺ antiporters. *Biochim Biophys Acta* **726**, 245-264
86. Aharonovitz, O., Demaurex, N., Woodside, M., and Grinstein, S. (1999) ATP dependence is not an intrinsic property of Na⁺/H⁺ exchanger NHE1: requirement for an ancillary factor. *Am J Physiol* **276**, C1303-1311
87. Pouyssegur, J., Chambard, J. C., Franchi, A., Paris, S., and Van Obberghen-Schilling, E. (1982) Growth factor activation of an amiloride-sensitive Na⁺/H⁺ exchange system in quiescent fibroblasts: coupling to ribosomal protein S6 phosphorylation. *Proc Natl Acad Sci U S A* **79**, 3935-3939
88. Wakabayashi, S., Hisamitsu, T., Pang, T., and Shigekawa, M. (2003) Kinetic dissection of two distinct proton binding sites in Na⁺/H⁺ exchangers by measurement of reverse mode reaction. *J Biol Chem* **278**, 43580-43585
89. Lacroix, J., Poet, M., Huc, L., Morello, V., Djerbi, N., Ragno, M., Rissel, M., Tekpli, X., Gounon, P., Lagadic-Gossmann, D., and Counillon, L. (2008) Kinetic analysis of the regulation of the Na⁺/H⁺ exchanger NHE-1 by osmotic shocks. *Biochemistry* **47**, 13674-13685

90. Monod, J., Wyman, J., and Changeux, J. P. (1965) On the Nature of Allosteric Transitions: A Plausible Model. *Journal of molecular biology* **12**, 88-118
91. Lacroix, J., Poet, M., Maehrel, C., and Counillon, L. (2004) A mechanism for the activation of the Na/H exchanger NHE-1 by cytoplasmic acidification and mitogens. *EMBO Rep* **5**, 91-96
92. Appel, M., Hizlan, D., Vinothkumar, K. R., Ziegler, C., and Kuhlbrandt, W. (2009) Conformations of NhaA, the Na/H Exchanger from Escherichia coli, in the pH-Activated and Ion-Translocating States. *Journal of molecular biology* **386**, 351-365
93. Olkhova, E., Hunte, C., Screpanti, E., Padan, E., and Michel, H. (2006) Multiconformation continuum electrostatics analysis of the NhaA Na⁺/H⁺ antiporter of Escherichia coli with functional implications. *Proceedings of the National Academy of Sciences of the United States of America* **103**, 2629-2634
94. Arkin, I. T., Xu, H. F., Jensen, M. O., Arbely, E., Bennett, E. R., Bowers, K. J., Chow, E., Dror, R. O., Eastwood, M. P., Flitman-Tene, R., Gregersen, B. A., Klepeis, J. L., Kolossvary, I., Shan, Y. B., and Shaw, D. E. (2007) Mechanism of Na⁺/H⁺ antiporting. *Science* **317**, 799-803
95. Pedersen, S. F., King, S. A., Nygaard, E. B., Rigor, R. R., and Cala, P. M. (2007) NHE1 inhibition by amiloride- and benzoylguanidine-type compounds. Inhibitor binding loci deduced from chimeras of NHE1 homologues with endogenous differences in inhibitor sensitivity. *J Biol Chem* **282**, 19716-19727
96. Khadilkar, A., Iannuzzi, P., and Orłowski, J. (2001) Identification of sites in the second exomembrane loop and ninth transmembrane helix of the mammalian Na⁺/H⁺ exchanger important for drug recognition and cation translocation. *J Biol Chem* **276**, 43792-43800
97. Counillon, L., Franchi, A., and Pouyssegur, J. (1993) A point mutation of the Na⁺/H⁺ exchanger gene (NHE1) and amplification of the mutated allele confer amiloride resistance upon chronic acidosis. *Proc Natl Acad Sci U S A* **90**, 4508-4512
98. Rupprecht, H. J., vom Dahl, J., Terres, W., Seyfarth, K. M., Richardt, G., Schultheis, H. P., Buerke, M., Sheehan, F. H., and Drexler, H. (2000) Cardioprotective effects of the Na⁽⁺⁾/H⁽⁺⁾ exchange inhibitor cariporide in patients with acute anterior myocardial infarction undergoing direct PTCA. *Circulation* **101**, 2902-2908
99. Theroux, P., Chaitman, B. R., Danchin, N., Erhardt, L., Meinertz, T., Schroeder, J. S., Tognoni, G., White, H. D., Willerson, J. T., and Jessel, A. (2000) Inhibition of the sodium-hydrogen exchanger with cariporide to prevent myocardial infarction in high-risk ischemic situations. Main results of the GUARDIAN trial. Guard during ischemia against necrosis (GUARDIAN) Investigators. *Circulation* **102**, 3032-3038
100. Le Gall, M., Grall, D., Chambard, J. C., Pouyssegur, J., and Van Obberghen-Schilling, E. (1998) An anchorage-dependent signal distinct from p42/44 MAP kinase activation is required for cell cycle progression. *Oncogene* **17**, 1271-1277

101. Vexler, Z. S., Symons, M., and Barber, D. L. (1996) Activation of Na⁺-H⁺ exchange is necessary for RhoA-induced stress fiber formation. *J Biol Chem* **271**, 22281-22284
102. Suh, B., Hille, B. (2005) Regulation of ion channels by phosphatidylinositol 4,5-bisphosphate. *Curr. Opin. Neurobiol.* **15**, 370-378
103. Goss, G. G., Woodside, M., Wakabayashi, S., Pouyssegur, J., Waddell, T., Downey, G. P., and Grinstein, S. (1994) ATP dependence of NHE-1, the ubiquitous isoform of the Na⁺/H⁺ antiporter. Analysis of phosphorylation and subcellular localization. *J. Biol. Chem.* **269**, 8741-8748
104. Aharonovitz, O., Zaun, H. C., Balla, T., York, J. D., Orłowski, J., and Grinstein, S. (2000) Intracellular pH regulation by Na⁽⁺⁾/H⁽⁺⁾ exchange requires phosphatidylinositol 4,5-bisphosphate. *J. Cell Biol.* **150**, 213-224
105. Aharonovitz, O., Zaun, H. C., Balla, T., York, J. D., Orłowski, J., and Grinstein, S. (2000) Intracellular pH regulation by Na⁽⁺⁾/H⁽⁺⁾ exchange requires phosphatidylinositol 4,5-bisphosphate. *The Journal of cell biology* **150**, 213-224
106. Pang, T., Wakabayashi, S., and Shigekawa, M. (2002) Expression of calcineurin B homologous protein 2 protects serum deprivation-induced cell death by serum-independent activation of Na⁺/H⁺ exchanger. *J Biol Chem* **277**, 43771-43777
107. Pang, T., Hisamitsu, T., Mori, H., Shigekawa, M., and Wakabayashi, S. (2004) Role of calcineurin B homologous protein in pH regulation by the Na⁺/H⁺ exchanger 1: tightly bound Ca²⁺ ions as important structural elements. *Biochemistry* **43**, 3628-3636
108. Pang, T., Su, X., Wakabayashi, S., and Shigekawa, M. (2001) Calcineurin homologous protein as an essential cofactor for Na⁺/H⁺ exchangers. *J Biol Chem* **276**, 17367-17372
109. Bertrand, B., Wakabayashi, S., Ikeda, T., Pouyssegur, J., and Shigekawa, M. (1994) The Na⁺/H⁺ exchanger isoform 1 (NHE1) is a novel member of the calmodulin-binding proteins. Identification and characterization of calmodulin-binding sites. *J Biol Chem* **269**, 13703-13709
110. Zaun, H. C., Shrier, A., and Orłowski, J. (2008) Calcineurin B homologous protein 3 promotes the Biosynthetic maturation, cell surface stability, and optimal transport of the Na⁺/H⁺ exchanger NHE1 isoform. *Journal of Biological Chemistry* **283**, 12456-12467
111. Li, X., Liu, Y., Alvarez, B. V., Casey, J. R., and Fliegel, L. (2006) A novel carbonic anhydrase II binding site regulates NHE1 activity. *Biochemistry* **45**, 2414-2424
112. Li, X., Alvarez, B., Casey, J. R., Reithmeier, R. A., and Fliegel, L. (2002) Carbonic anhydrase II binds to and enhances activity of the Na⁺/H⁺ exchanger. *J Biol Chem* **277**, 36085-36091
113. Denker, S. P., and Barber, D. L. (2002) Cell migration requires both ion translocation and cytoskeletal anchoring by the Na-H exchanger NHE1. *The Journal of cell biology* **159**, 1087-1096
114. Denker, S. P., Huang, D. C., Orłowski, J., Furthmayr, H., and Barber, D. L. (2000) Direct binding of the Na⁻-H exchanger NHE1 to ERM proteins regulates the

- cortical cytoskeleton and cell shape independently of H(+) translocation. *Mol Cell* **6**, 1425-1436
115. Grinstein, S., Rotin, D., and Mason, M. J. (1989) Na⁺/H⁺ exchange and growth factor-induced cytosolic pH changes. Role in cellular proliferation. *Biochim Biophys Acta* **988**, 73-97
 116. Shrode, L., Cabado, A., Goss, G., and Grinstein, S. (1996) Role of the Na⁺/H⁺ antiporter isoforms in cell volume regulation. In *The Na⁺/H⁺ Exchanger*, Edited by L. Fliegel, R.G. Landes Company, 101-122
 117. Krump, E., Nikitas, K., and Grinstein, S. (1997) Induction of tyrosine phosphorylation and Na⁺/H⁺ exchanger activation during shrinkage of human neutrophils. *J Biol Chem* **272**, 17303-17311
 118. Demaurex, N., and Grinstein, S. (1994) Na⁺/H⁺ antiport: modulation by ATP and role in cell volume regulation. *J Exp Biol* **196**, 389-404
 119. Su, X., Pang, T., Wakabayashi, S., and Shigekawa, M. (2003) Evidence for involvement of the putative first extracellular loop in differential volume sensitivity of the Na⁺/H⁺ exchangers NHE1 and NHE2. *Biochemistry* **42**, 1086-1094
 120. Ladoux, A., Miglierina, R., Krawice, I., Cragoe, E. J., Jr., Abita, J. P., and Frelin, C. (1988) Single-cell analysis of the intracellular pH and its regulation during the monocytic differentiation of U937 human leukemic cells. *Eur J Biochem* **175**, 455-460
 121. Li, X., Karki, P., Lei, L., Wang, H., and Fliegel, L. (2009) Na⁺/H⁺ exchanger isoform 1 facilitates cardiomyocyte embryonic stem cell differentiation. *Am J Physiol Heart Circ Physiol* **296**, H159-170
 122. Rieder, C. V., and Fliegel, L. (2003) Transcriptional regulation of Na⁺/H⁺ exchanger expression in the intact mouse. *Mol Cell Biochem* **243**, 87-95
 123. Yang, W., Dyck, J. R., and Fliegel, L. (1996) Regulation of NHE1 expression in L6 muscle cells. *Biochim Biophys Acta* **1306**, 107-113
 124. Pouyssegur, J., Sardet, C., Franchi, A., L'Allemain, G., and Paris, S. (1984) A specific mutation abolishing Na⁺/H⁺ antiport activity in hamster fibroblasts precludes growth at neutral and acidic pH. *Proc Natl Acad Sci U S A* **81**, 4833-4837
 125. Stock, C., and Schwab, A. (2006) Role of the Na/H exchanger NHE1 in cell migration. *Acta Physiol (Oxf)* **187**, 149-157
 126. Grinstein, S., Woodside, M., Waddell, T. K., Downey, G. P., Orłowski, J., Pouyssegur, J., Wong, D. C., and Foskett, J. K. (1993) Focal localization of the NHE-1 isoform of the Na⁺/H⁺ antiport: assessment of effects on intracellular pH. *The EMBO journal* **12**, 5209-5218
 127. Klein, M., Seeger, P., Schuricht, B., Alper, S. L., and Schwab, A. (2000) Polarization of Na(+)/H(+) and Cl(-)/HCO₃(-) exchangers in migrating renal epithelial cells. *J Gen Physiol* **115**, 599-608
 128. Busco, G., Cardone, R. A., Greco, M. R., Bellizzi, A., Colella, M., Antelmi, E., Mancini, M. T., Dell'Aquila, M. E., Casavola, V., Paradiso, A., and Reshkin, S. J. (2010) NHE1 promotes invadopodial ECM proteolysis through acidification of the peri-invadopodial space. *FASEB J* **24**, 3903-3915

129. Stock, C., Cardone, R. A., Busco, G., Krahling, H., Schwab, A., and Reshkin, S. J. (2008) Protons extruded by NHE1: digestive or glue? *European journal of cell biology* **87**, 591-599
130. Harguindey, S., Orive, G., Luis Pedraz, J., Paradiso, A., and Reshkin, S. J. (2005) The role of pH dynamics and the Na⁺/H⁺ antiporter in the etiopathogenesis and treatment of cancer. Two faces of the same coin--one single nature. *Biochim Biophys Acta* **1756**, 1-24
131. Paradiso, A., Cardone, R. A., Bellizzi, A., Bagorda, A., Guerra, L., Tommasino, M., Casavola, V., and Reshkin, S. J. (2004) The Na⁺-H⁺ exchanger-1 induces cytoskeletal changes involving reciprocal RhoA and Rac1 signaling, resulting in motility and invasion in MDA-MB-435 cells. *Breast Cancer Res* **6**, R616-628
132. Lagarde, A. E., Franchi, A. J., Paris, S., and Pouyssegur, J. M. (1988) Effect of mutations affecting Na⁺: H⁺ antiport activity on tumorigenic potential of hamster lung fibroblasts. *J Cell Biochem* **36**, 249-260
133. He, B., Deng, C., Zhang, M., Zou, D., and Xu, M. (2007) Reduction of intracellular pH inhibits the expression of VEGF in K562 cells after targeted inhibition of the Na⁺/H⁺ exchanger. *Leukemia research* **31**, 507-514
134. Yang, X., Wang, D., Dong, W., Song, Z., and Dou, K. (2010) Inhibition of Na⁽⁺⁾/H⁽⁺⁾ exchanger 1 by 5-(N-ethyl-N-isopropyl) amiloride reduces hypoxia-induced hepatocellular carcinoma invasion and motility. *Cancer Lett* **295**, 198-204
135. Kato, Y., Lambert, C. A., Colige, A. C., Mineur, P., Noel, A., Frankenne, F., Foidart, J. M., Baba, M., Hata, R., Miyazaki, K., and Tsukuda, M. (2005) Acidic extracellular pH induces matrix metalloproteinase-9 expression in mouse metastatic melanoma cells through the phospholipase D-mitogen-activated protein kinase signaling. *J Biol Chem* **280**, 10938-10944
136. Koblinski, J. E., Ahram, M., and Sloane, B. F. (2000) Unraveling the role of proteases in cancer. *Clin Chim Acta* **291**, 113-135
137. Anderson, S. E., Kirkland, D. M., Beyschau, A., and Cala, P. M. (2005) Acute effects of 17beta-estradiol on myocardial pH, Na⁺, and Ca²⁺ and ischemia-reperfusion injury. *American journal of physiology* **288**, C57-64
138. Piper, H. M., Meuter, K., and Schafer, C. (2003) Cellular mechanisms of ischemia-reperfusion injury. *Ann Thorac Surg* **75**, S644-648
139. Avkiran, M., Gross, G., Karmazyn, M., Klein, H., Murphy, E., and Ytrehus, K. (2001) Na⁺/H⁺ exchange in ischemia, reperfusion and preconditioning. *Cardiovasc Res* **50**, 162-166
140. Murphy, E., Cross, H. R., and Steenbergen, C. (2002) Is Na/Ca exchange during ischemia and reperfusion beneficial or detrimental? *Annals of the New York Academy of Sciences* **976**, 421-430
141. Karmazyn, M., Liu, Q., Gan, X. T., Brix, B. J., and Fliegel, L. (2003) Aldosterone increases NHE-1 expression and induces NHE-1-dependent hypertrophy in neonatal rat ventricular myocytes. *Hypertension* **42**, 1171-1176
142. Fliegel, L. (2001) Regulation of myocardial Na⁺/H⁺ exchanger activity. *Basic Res Cardiol* **96**, 301-305

143. Mentzer, R. M., Jr., Lasley, R. D., Jessel, A., and Karmazyn, M. (2003) Intracellular sodium hydrogen exchange inhibition and clinical myocardial protection. *Ann Thorac Surg* **75**, S700-S708
144. Lang, H. J. (2003) Chemistry of NHE inhibitors. p 239-253, in *The Na⁺/H⁺ Exchanger, From Molecular to Its Role in Disease*, edited by M. Karmazyn, M. Avkiran and L. Fliegel, Kluwer academic Publishers, Boston/Dordrecht/London, 318p.
145. Murphy, E., and Allen, D. G. (2009) Why did the NHE inhibitor clinical trials fail? *J Mol Cell Cardiol* **46**, 137-141
146. Counillon, L., Noel, J., Reithmeier, R. A., and Pouyssegur, J. (1997) Random mutagenesis reveals a novel site involved in inhibitor interaction within the fourth transmembrane segment of the Na⁺/H⁺ exchanger-1. *Biochemistry* **36**, 2951-2959
147. Touret, N., Poujeol, P., and Counillon, L. (2001) Second-site revertants of a low-sodium-affinity mutant of the Na⁺/H⁺ exchanger reveal the participation of TM4 into a highly constrained sodium-binding site. *Biochemistry* **40**, 5095-5101
148. Ding, J., Ng, R. W., and Fliegel, L. (2007) Functional characterization of the transmembrane segment VII of the NHE1 isoform of the Na⁺/H⁺ exchanger. *Canadian journal of physiology and pharmacology* **85**, 319-325
149. Ikeda, T., Schmitt, B., Pouyssegur, J., Wakabayashi, S., and Shigekawa, M. (1997) Identification of cytoplasmic subdomains that control pH-sensing of the Na⁺/H⁺ exchanger (NHE1): pH-maintenance, ATP-sensitive, and flexible loop domains. *J Biochem* **121**, 295-303
150. Wakabayashi, S., Hisamitsu, T., Pang, T., and Shigekawa, M. (2003) Mutations of Arg440 and Gly455/Gly456 oppositely change pH sensing of Na⁺/H⁺ exchanger 1. *J Biol Chem* **278**, 11828-11835
151. Slepko, E. R., Chow, S., Lemieux, M. J., and Fliegel, L. (2004) Proline residues in transmembrane segment IV are critical for activity, expression and targeting of the Na⁺/H⁺ exchanger isoform 1. *Biochem J* **379**, 31-38
152. Wakabayashi, S., Pang, T., Su, X., and Shigekawa, M. (2000) Second mutations rescue point mutant of the Na(+)/H(+) exchanger NHE1 showing defective surface expression. *FEBS letters* **487**, 257-261
153. Munoz, V., Blanco, F. J., and Serrano, L. (1995) The hydrophobic-staple motif and a role for loop-residues in alpha-helix stability and protein folding. *Nat Struct Biol* **2**, 380-385
154. Zhao, M. M., Gaivin, R. J., and Perez, D. M. (1998) The third extracellular loop of the beta2-adrenergic receptor can modulate receptor/G protein affinity. *Molecular pharmacology* **53**, 524-529
155. Herz, K., Rimon, A., Jeschke, G., and Padan, E. (2009) beta-Sheet-dependent Dimerization Is Essential for the Stability of NhaA Na⁺/H⁺ Antiporter. *Journal of Biological Chemistry* **284**, 6337-6347
156. Rimon, A., Tzubery, T., and Padan, E. (2007) Monomers of the NhaA Na⁺/H⁺ antiporter of Escherichia coli are fully functional yet dimers are beneficial under extreme stress conditions at alkaline pH in the presence of Na⁺ or Li⁺. *Journal of Biological Chemistry* **282**, 26810-26821

157. Murtazina, R., Booth, B. J., Bullis, B. L., Singh, D. N., and Fliegel, L. (2001) Functional analysis of polar amino-acid residues in membrane associated regions of the NHE1 isoform of the mammalian Na⁺/H⁺ exchanger. *European Journal of Biochemistry* **268**, 4674-4685
158. Khadilkar, A., Iannuzzi, P., and Orłowski, J. (2001) Identification of sites in the second exomembrane loop and ninth transmembrane helix of the mammalian Na⁺/H⁺ exchanger important for drug recognition and cation translocation. *Journal of Biological Chemistry* **276**, 43792-43800
159. Wang, J., Sahoo, D., Sykes, B. D., and Ryan, R. O. (1998) NMR evidence for a conformational adaptation of apolipoprotein III upon lipid association. *Biochemistry and cell biology = Biochimie et biologie cellulaire* **76**, 276-283
160. Slepko, E. R., Rainey, J. K., Sykes, B. D., and Fliegel, L. (2007) Structural and functional analysis of the Na⁽⁺⁾/H⁽⁺⁾ exchanger. *Biochem J* **401**, 623-633
161. Murtazina, R., Booth, B. J., Bullis, B. L., Singh, D. N., and Fliegel, L. (2001) Functional analysis of polar amino-acid residues in membrane associated regions of the NHE1 isoform of the mammalian Na⁺/H⁺ exchanger. *Eur J Biochem* **268**, 4674-4685
162. Lee, B. L., Li, X., Liu, Y., Sykes, B. D., and Fliegel, L. (2009) Structural and functional analysis of extracellular loop 2 of the Na⁽⁺⁾/H⁽⁺⁾ exchanger. *Biochim Biophys Acta* **1788**, 2481-2488
163. Khadilkar, A., Iannuzzi, P., and Orłowski, J. (2001) Identification of sites in the second exomembrane loop and ninth transmembrane helix of the mammalian Na⁺/H⁺ exchanger important for drug recognition and cation translocation. *J Biol Chem* **276**, 43792-43800
164. Hisamitsu, T., Yamada, K., Nakamura, T. Y., and Wakabayashi, S. (2007) Functional importance of charged residues within the putative intracellular loops in pH regulation by Na⁺/H⁺ exchanger NHE1. *The FEBS journal* **274**, 4326-4335
165. Rimon, A., Tzuber, T., and Padan, E. (2007) Monomers of the NhaA Na⁺/H⁺ antiporter of Escherichia coli are fully functional yet dimers are beneficial under extreme stress conditions at alkaline pH in the presence of Na⁺ or Li⁺. *J Biol Chem* **282**, 26810-26821
166. Olami, Y., Rimon, A., Gerchman, Y., Rothman, A., and Padan, E. (1997) Histidine 225, a residue of the NhaA-Na⁺/H⁺ antiporter of Escherichia coli is exposed and faces the cell exterior. *J Biol Chem* **272**, 1761-1768
167. Slepko, E. R., Rainey, J. K., Li, X., Liu, Y., Cheng, F. J., Lindhout, D. A., Sykes, B. D., and Fliegel, L. (2005) Structural and functional characterization of transmembrane segment IV of the NHE1 isoform of the Na⁺/H⁺ exchanger. *J Biol Chem* **280**, 17863-17872
168. Amith, S. R., and Fliegel, L. (2017) Na⁺/H⁺ exchanger-mediated hydrogen ion extrusion as a carcinogenic signal in triple-negative breast cancer etiopathogenesis and prospects for its inhibition in therapeutics. *Seminars in cancer biology* **43**, 35-41
169. Slepko, E., Ding, J., Han, J., and Fliegel, L. (2007) Mutational analysis of potential pore-lining amino acids in TM IV of the Na⁽⁺⁾/H⁽⁺⁾ exchanger. *Biochim Biophys Acta* **1768**, 2882-2889

170. Fagerland, M. W., and Sandvik, L. (2009) The Wilcoxon-Mann-Whitney test under scrutiny. *Stat Med* **28**, 1487-1497
171. Guntert, P., Mumenthaler, C., and Wuthrich, K. (1997) Torsion angle dynamics for NMR structure calculation with the new program DYANA. *Journal of molecular biology* **273**, 283-298
172. Delaglio, F., Grzesiek, S., Vuister, G. W., Zhu, G., Pfeifer, J., and Bax, A. (1995) NMRPipe: a multidimensional spectral processing system based on UNIX pipes. *J Biomol NMR* **6**, 277-293
173. Johnson, B. A., and Blevins, R. A. (1994) NMR View: A computer program for the visualization and analysis of NMR data. *J Biomol NMR* **4**, 603-614
174. Johnson, B. A., and Blevins, R. A. (1994) NMRView: A computer program for the visualization and analysis of NMR data. *J Biomol NMR* **4**, 603-614
175. Ordog, R. (2008) PyDeT, a PyMOL plug-in for visualizing geometric concepts around proteins. *Bioinformatics* **2**, 346-347
176. Fleming, K. G., and Engelman, D. M. (2001) Specificity in transmembrane helix-helix interactions can define a hierarchy of stability for sequence variants. *Proc Natl Acad Sci U S A* **98**, 14340-14344
177. Wakabayashi, S., Pang, T., Su, X., and Shigekawa, M. (2000) Second mutations rescue point mutant of the Na(+)/H(+) exchanger NHE1 showing defective surface expression. *FEBS letters* **487**, 257-261
178. Wakabayashi, S., Hisamitsu, T., Pang, T., and Shigekawa, M. (2003) Mutations of Arg440 and Gly455/Gly456 oppositely change pH sensing of Na⁺/H⁺ exchanger 1. *J Biol Chem* **278**, 11828-11835
179. Haynes, W. M. (2011). *CRC handbook of Chemistry and Physics, 92st ed.*; Haynes, W. M., Editor; CRC Press: Boca Raton, FL,
180. Bordag, N., and Keller, S. (2010) Alpha-helical transmembrane peptides: a "divide and conquer" approach to membrane proteins. *Chemistry and physics of lipids* **163**, 1-26
181. Katragadda, M., Alderfer, J. L., and Yeagle, P. L. (2000) Solution structure of the loops of bacteriorhodopsin closely resembles the crystal structure. *Biochim Biophys Acta* **1466**, 1-6
182. Lee, B. L., Liu, Y., Li, X., Sykes, B. D., and Fliegel, L. (2012) Structural and functional analysis of extracellular loop 4 of the Nhe1 isoform of the Na(+)/H(+) exchanger. *Biochim Biophys Acta* **1818**, 2783-2790
183. Warschawski, D. E., Arnold, A. A., Beaugrand, M., Gravel, A., Chartrand, E., and Marcotte, I. (2011) Choosing membrane mimetics for NMR structural studies of transmembrane proteins. *Biochim Biophys Acta* **1808**, 1957-1974